The Journal of Experimental Biology 213, 4110-4122

doi:10.1242/jeb.043091

The effect of body size on the wing movements of pteropodid bats, with insights into thrust and lift production

Daniel K. Riskin[1,*], José Iriarte-Díaz[2], Kevin M. Middleton[3], Kenneth S. Breuer[4] and Sharon M. Swartz[1,4]

[1]Department of Ecology and Evolutionary Biology, Brown University, Providence, RI 02912, USA, [2]Department of Organismal Biology and Anatomy, The University of Chicago, Chicago, IL 60637, USA, [3]Department of Biology, California State University San Bernardino, San Bernardino, CA 92407, USA and [4]School of Engineering, Brown University, Providence, RI 02912, USA

*Author for correspondence at present address: Department of Biology, City College of the City University of New York, New York, NY 10031, USA (driskin@ccny.cuny.edu)

Accepted 26 July 2010

SUMMARY

In this study we compared the wing kinematics of 27 bats representing six pteropodid species ranging more than 40 times in body mass (M_b=0.0278–1.152 kg), to determine whether wing posture and overall wing kinematics scaled as predicted according to theory. The smallest species flew in a wind tunnel and the other five species in a flight corridor. Seventeen kinematic markers on the midline and left side of the body were tracked in three dimensions. We used phylogenetically informed reduced major axis regression to test for allometry. We found that maximum wingspan (b_{max}) and maximum wing area (S_{max}) scaled with more positive allometry, and wing loading (Q_s) with more negative allometry ($b_{max} \propto M_b^{0.423}$; $S_{max} \propto M_b^{0.768}$; $Q_s \propto M_b^{0.233}$) than has been reported in previous studies that were based on measurements from specimens stretched out flat on a horizontal surface. Our results suggest that larger bats open their wings more fully than small bats do in flight, and that for bats, body measurements alone cannot be used to predict the conformation of the wings in flight. Several kinematic variables, including downstroke ratio, wing stroke amplitude, stroke plane angle, wing camber and Strouhal number, did not change significantly with body size, demonstrating that many aspects of wing kinematics are similar across this range of body sizes. Whereas aerodynamic theory suggests that preferred flight speed should increase with mass, we did not observe an increase in preferred flight speed with mass. Instead, larger bats had higher lift coefficients (C_L) than did small bats ($C_L \propto M_b^{0.170}$). Also, the slope of the wingbeat period (T) to body mass regression was significantly more shallow than expected under isometry ($T \propto M_b^{0.180}$), and angle of attack (α) increased significantly with body mass [$\alpha \propto \log(M_b)7.738$]. None of the bats in our study flew at constant speed, so we used multiple regression to isolate the changes in wing kinematics that correlated with changes in flight speed, horizontal acceleration and vertical acceleration. We uncovered several significant trends that were consistent among species. Our results demonstrate that for medium- to large-sized bats, the ways that bats modulate their wing kinematics to produce thrust and lift over the course of a wingbeat cycle are independent of body size.

Supplementary material available online at http://jeb.biologists.org/cgi/content/full/213/23/4110/DC1

Key words: allometry, bats, *Cynopterus brachyotis*, *Eidolon helvum*, flight, isometry, kinematics, *Pteropus hypomelanus*, *Pteropus pumilus*, *Pteropus vampyrus*, *Rousettus aegyptiacus*, scaling.

INTRODUCTION

Body size governs almost every aspect of animal biology. Many fundamental aspects of ontogeny, physiology, ecology and behavior can be largely predicted with little more information than the mass of an animal. These, and many other important aspects of an organism's life, scale predictably with body mass, according to fundamental form–function relationships (Brown and West, 2000; Dial et al., 2008). The influence of body size on locomotion is no less striking, and biomechanical investigations have revealed that just as body shape changes with size, so too do locomotor kinematics (Biewener, 1983; Biewener, 2005; Heglund and Taylor, 1988).

Part of the reason that animals of different sizes move their bodies differently is that the physical demands of locomotion change with body size. As an extreme example, small flying animals moving through the air must deal with high viscous forces relative to inertial forces, whereas for larger flying animals, viscous forces are much smaller than inertial ones. As a result, a <100 μg wasp uses constant clap and fling wing motions to fly whereas a 10 kg Andean condor travels mostly by simply holding its wings outstretched (Ellington, 1999; McGahan, 1973; Miller and Peskin, 2005). Within the range of body sizes between those extremes, animal flight can differ in subtle but important ways. The mechanics of insect flight differ between fruit flies and hawkmoths, and the way a bird flies also varies from hummingbirds to pigeons to vultures (Combes and Daniel, 2003; Dial and Biewener, 1993; Dickinson and Götz, 1996; Sane, 2003; McGahan, 1973; Warrick et al., 2005). Unlike insects and birds, however, bats have largely been assumed to use similar mechanisms of aerodynamic force production in flight, regardless of size (Bullen and McKenzie, 2002; Hedenström et al., 2007; Norberg and Rayner, 1987), even though bats range in body mass over roughly three orders of magnitude, from the ≤0.002 kg bumblebee bat (*Craseonycteris thonglongyai*) to >1.2 kg flying foxes (*Pteropus* spp.) (Hill and Smith, 1981; Kunz and Jones, 2000; Surlykke et al., 1993).

The purpose of this study is to examine the influence of body size on wing kinematics in bats. The body shapes and foraging modes of bats vary widely among families, so we focused on a single family, the Pteropodidae. This family consists of ca. 186 species distributed throughout the paleotropics (Wilson and Reeder, 2005) and is characterized by fruit and nectar-feeding, non-echolocating

animals that are ecologically and morphologically similar across a broad range of body sizes. No other chiropteran family possesses so wide a range of body sizes as the pteropodids (Nowak, 1994).

We investigated wing posture, wing kinematics and the patterns with which kinematics change with flight velocity. In this study we also examined the influences of horizontal and vertical accelerations on wing kinematics, as a means of studying how the kinematics of bats reflect aeromechanical force production in those directions.

MATERIALS AND METHODS

Video recordings and kinematic reconstructions

Flight recordings and calibrations

We recorded the flight kinematics of 27 animals from six species ranging more than 40-fold in body mass, from 0.0278 kg to 1.152 kg (Table 1). Bats of the smallest species, *Cynopterus brachyotis*, were flown in a 1.4 m×1.2 m×1.2 m (L×W×H) wind tunnel at the Concord Field Station of Harvard University in Bedford MA, USA (Hedrick et al., 2002). Bats belonging to the other five species were flown in a 14.5 m×2.8 m×2.4 m (L×W×H) flight corridor at the Lubee Bat Conservancy in Gainesville FL, USA. Bats were recorded at 1000 Hz using three phase-locked Photron 1024 PCI digital high-speed cameras (Photron USA, Inc., San Diego, CA USA). A fourth phase-locked 1000 Hz camera, a Photron APX, was also used to record corridor flights. All cameras had 1024×1024 pixel resolution.

Before experiments, each bat was anesthetized with isoflurane gas then marked with non-toxic acrylic paint at 17 anatomical landmarks on the fur and skin of the sagittal midline and the left half of the body (Fig. 1A). At least ten flights were recorded from each individual, but only five flights per individual were used for analyses. Those five were selected to sample the broadest range possible of flight velocities for each individual.

The volumes through which bats flew were calibrated using the direct linear transformation (DLT) method (Abdel-Aziz and Karara, 1971), based on a 0.35 m×0.35 m×0.28 m (L×W×H) calibration frame for the wind tunnel trials, and on a series of vertical wires and beads for the corridor experiments, spanning 2.00 m× 1.25 m×2.40 m (L×W×H).

Marker tracking and coordinate systems

The positions of 17 anatomical markers were digitized in each video frame (Fig. 1). Where a marker was visible in two or more cameras at a given instant, its position could be calculated using the DLT method. In those frames where a marker was not visible to at least two cameras, its position was interpolated based on its three-dimensional positions before and after that interval, using an over-constrained least-squares polynomial fit of its trajectory. For contiguous gaps in the data with rich data at the end points, a third-order polynomial was used, and for gaps with sporadic intermediate points, a sixth-order polynomial was used (Riskin et al., 2008). The interpolations were visually checked for all 17 markers in all 135 trials by superimposing the interpolated three-dimensional path on the original movies. The wing membrane was modeled as a series of 18 flat triangles spanning the *xyz* coordinates of the markers (Fig. 1A).

For the purposes of this study, we define a body-centered coordinate system (x_b, y_b, z_b) and a global coordinate system (x_g, y_g, z_g) (Gatesy and Baier, 2005). Both are right-handed, and in both, x and y are horizontal and z is vertical (Fig. 1B,C). The global coordinates represent the motion of the bat relative to still air, with positive x_g in the direction of travel, positive y_g to the bat's left and positive z_g pointing vertical up. To obtain global coordinates for corridor trials, we calculated the positions of the 17 markers throughout the trial relative to the calibration frame, then rotated the coordinate system so that the bat's anterior sternum marker (*a* in Fig. 1A) moved forward in the x_g direction, beginning and ending the wingbeat cycle at the same y_g value. We then subtracted the initial position of the anterior sternum marker from all positions. Thus, every trial began with the anterior sternum marker at (x_g, y_g, z_g)=(0, 0, 0), and ended with the sternum at some positive x_g position with y_g=0. Global coordinates for wind-tunnel trials were calculated analogously but were adjusted to correct for the velocity and direction of the air so that the global coordinates would also represent the motion of the bat's body relative to still air.

The body-centered coordinate system was calculated from the global coordinates by subtracting the position of the anterior sternum marker in each time step from the positions of all markers in that time step. The net effect was that the anterior sternum marker remained at (x_b, y_b, z_b)=(0, 0, 0) throughout the trial and the head faced positive x_b (Fig. 1B).

We restricted our analyses from each flight to a single wingbeat cycle. Where possible (88 of 135 trials), the upper reversal points of the wrist marker in the z_b direction were used to denote the beginning and end of the wingbeat cycle (Fig. 1B). For some flight corridor trials, a complete wingbeat cycle occurred within the calibrated volume, but not spanning those endpoints. In those cases, we used, in order of preference, the lower reversal points of the wrist (38 of 135), the upper reversal points of the wingtip (6 of 135), or the lower reversal points of the wingtip (3 of 135).

Measurements of body shape and posture

To determine how wing shape changed with body mass (M_b), we extracted information about three-dimensional wing conformation from the kinematic recordings. Whereas morphometric measurements are typically taken from specimens with wings extended on a flat surface, our methods capture posture, one of the most important aspects of wing form for understanding flight mechanics (Nudds, 2007). The following parameters were calculated from each trial.

Maximum wingspan (b_{max}): two times the maximum distance of the wingtip marker from the mid-sagittal plane (y_b=0) in a trial. This always occurred during the downstroke.

Minimum wingspan (b_{min}): for each time step we found the y_b-value of the wing marker furthest from the y_b=0 plane. The b_{min}

Table 1. Body mass of the 27 individuals used in the present study, and experimental flight conditions

Species name	Abbreviation	Colour code	Body mass (kg)	Flight conditions
Cynopterus brachyotis (Müller)	*Cb*	Purple	0.028, 0.031, 0.035, 0.035, 0.040	Wind tunnel
Rousettus aegyptiacus (É. Geoffroy)	*Ra*	Blue	0.112, 0.132, 0.159	Flight corridor
Pteropus pumilus Miller	*Pp*	Green	0.178, 0.178, 0.180, 0.204, 0.212	Flight corridor
Eidolon helvum (Kerr)	*Eh*	Yellow	0.254, 0.266, 0.278, 0.326, 0.332	Flight corridor
Pteropus hypomelanus Temminck	*Ph*	Orange	0.454, 0.464, 0.468, 0.490, 0.526	Flight corridor
Pteropus vampyrus Linnaeus	*Pv*	Red	1.020, 1.052, 1.090, 1.152	Flight corridor

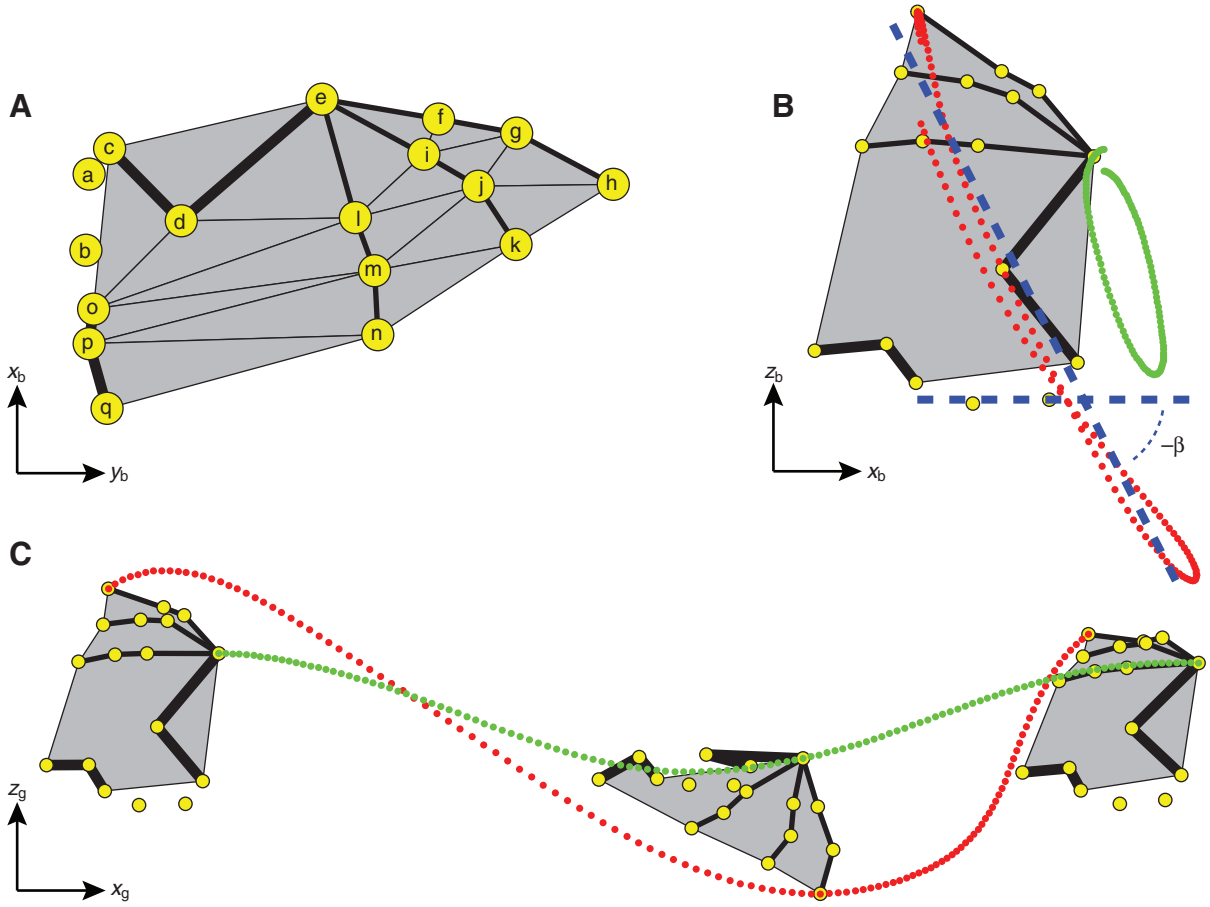

Fig. 1. (A) Ventral view of a bat's left wing; 17 markers were painted on the bat, then tracked in numerous camera views. Markers used were: anterior and posterior sternum (a and b, respectively), shoulder (c), elbow (d), wrist (e), the metacarpophalangeal and interphalangeal joints and tips of digits III (f, g, h), IV (i, j, k), and V (l, m, n), the hip (o), knee (p) and foot (q). (B) Right lateral view of a bat in the body-centered coordinate system, with the left wing shown in grey. The path of the wrist (green dots) and wingtip (red dots) over a wingbeat cycle are shown. Stroke plane angle (β) was calculated as the angle between horizontal and the reduced major axis regression best fit line of the wingtip path in the x_b–z_b plane (blue dashed lines). By convention, β is expressed as a negative number (Norberg, 1990). (C) Right lateral view of the bat in the global coordinate system, with the paths of the wrist (green dots) and wingtip (red dots) over the wingbeat cycle shown. The position and posture of the left wing are shown at three time points in the wingbeat cycle.

value for a trial was the smallest of those values across the entire wingbeat cycle, multiplied by two. This always occurred during the upstroke.

Maximum wing chord (c_{max}): the greatest two-dimensional distance in a trial between the wrist and the tip of digit V (*e* and *n* in Fig. 1A, respectively), using their x_b and z_b position data only, and ignoring y_b.

Maximum wing area (S_{max}): the left wing was divided into 18 triangular surfaces (Fig. 1A). The areas of those triangles were summed, then multiplied by two, to arrive at total wing area (S). The result is a coarse three-dimensional mesh which approximates the wetted area, not a two-dimensional projection. This was done for each time step over the course of the wingbeat cycle, and S_{max} was the maximum value of S for a trial. We chose this method because it uses our high-fidelity measurements to arrive at a more detailed index of wing conformation than would a two-dimensional projected area.

Wing loading (Q_s): defined as:

$$Q_s = \frac{M_b \boldsymbol{g}}{S_{max}} , \quad (1)$$

where $\boldsymbol{g}$ is the acceleration of gravity (9.81 m s^{-2}).

Aspect ratio (AR): defined as:

$$AR = \frac{b_{max}^2}{S_{max}} . \quad (2)$$

Measurements of velocity and acceleration

Parameters were calculated as follows.

Horizontal velocity (V_{horiz}): the horizontal distance traveled by the anterior sternum marker over the course of the wingbeat cycle, divided by the duration of the wingbeat cycle.

Vertical velocity (V_{vert}): the vertical distance traveled by the anterior sternum marker over the course of the wingbeat cycle, divided by the duration of the wingbeat cycle.

Horizontal acceleration (A_{horiz}): the change in forward velocity between the beginning of the wingbeat cycle and the end of the wingbeat cycle, divided by the duration of the wingbeat cycle. Both estimates of forward velocity were calculated using the slope of a linear fit of the anterior sternum marker's x_g position over time, using a 4 ms window. Since the posture of the bat was roughly the same at the beginning and end of a wingbeat cycle, inertial effects can be neglected, so the change in speed of the sternum markers approximates the change in the speed of the center of mass.

Vertical acceleration (A_{vert}): calculated analogously to A_{horiz}, but using z_g position over time instead of x_g.

Measurements of wing kinematics

The following parameters were obtained.

Wingbeat period (T): the time taken to complete the wingbeat cycle.

Downstroke duration (T_{down}): the duration of the downstroke, based on the motion of the wrist in z_b dimension.

Downstroke ratio (τ): the proportion of the wingbeat cycle duration occupied by the downstroke, calculated as:

$$\tau = \frac{T_{down}}{T} . \quad (3)$$

Wing stroke amplitude (ϕ): the maximum three-dimensional angle between any two positions of the wrist relative to the shoulder within a wingbeat cycle.

Strouhal number (St): a dimensionless descriptor of flapping motion, calculated using the distance traveled by the wingtip in the z_b direction:

$$\frac{(z_{b,wingtip})_{max} - (z_{b,wingtip})_{min}}{TV_{horiz}} . \quad (4)$$

Stroke plane angle (β): the trajectory of the wingtip in the x_b–z_b plane was fitted to a linear function using orthogonal regression. The angle between that regression line and horizontal was multiplied by –1 to calculate β, which is negative by convention (Norberg, 1990) (Fig. 1B).

Wing camber at maximum wingspan: in the time step (camera frame) corresponding to b_{max}, which always occurred at some time during the downstroke, a parasagittal (x_g–z_g) cross section of the wing at the y_g value of the wrist was made. The straight line from the wrist to trailing edge was defined as the chord line. Of the 18 triangular sections of the modeled wing, exactly six always intersected that plane at the time of b_{max} (Fig. 2A), resulting in seven intersections of a triangle border and the plane. The first term of a sine series was fitted to those seven intersection points to create a curved line between the wrist and the trailing edge of the wing that came as close to those seven points as possible. To calculate wing camber, we divided the maximum distance to the chord line from that curve by the length of the chord line (Fig. 2B). Our estimate of camber is an instantaneous value for a dynamically changing parameter, and although it might not represent the maximum or even average camber over the whole wingbeat cycle, it is a value that can be defined in a clear, unambiguous manner for ease of comparison among wingbeat cycles.

Angle of attack (α): the angle of the wing chord relative to the incoming flow of air was calculated at the instant of maximum wingspan, in the same time step as wing camber was calculated. The chord line was defined as a straight line between the wrist and the intersection of the trailing edge with the x_g–z_g plane of the wrist (Fig. 2C). The angle of the chord line above horizontal was defined

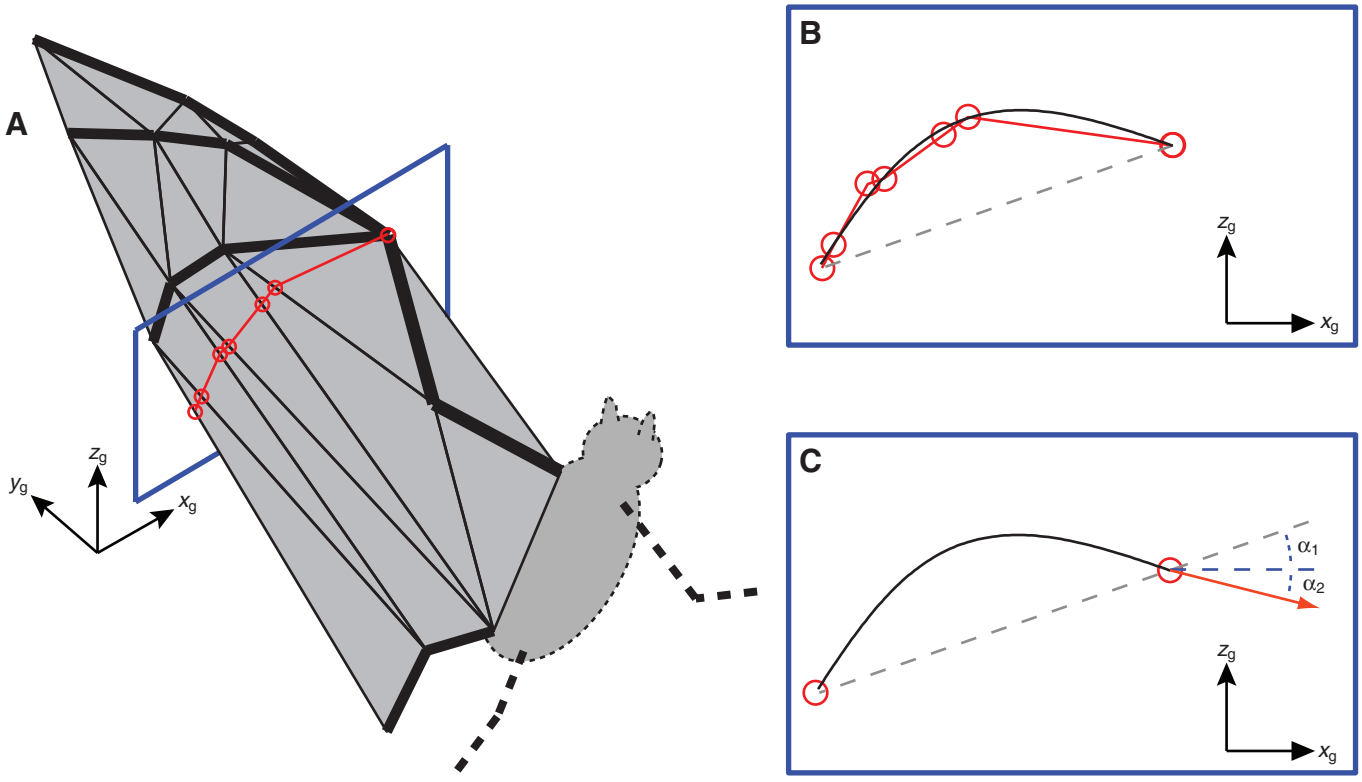

Fig. 2. Mid-downstroke wing camber and angle of attack were estimated as follows: (A) A parasagittal (x_g–z_g) cross section of the wing was taken at the y_g-value of the wrist at the time of maximum wingspan. Six triangular sections of the wing membrane crossed that plane and the intersections of triangle borders in the plane (red circles) were used as estimates of membrane position. (B) The actual curved shape of the membrane in the plane (solid black line) was estimated using the first term of a sine series fitted to those seven points. The maximum distance of the membrane line from the chord line (dashed grey line) was divided by the length of the chord line to give wing camber. (C) Angle of attack (α) was calculated as $\alpha_1 + \alpha_2$, where α_1 is the angle of the wing chord line above horizontal (blue dashed line), and α_2 is the angle between horizontal and the velocity vector of the wrist (red arrow) in the x_g–z_g plane.

as α_1. The angle velocity vector of the wrist below horizontal in the x_g–z_g plane, was defined as α_2. Angle of attack (α) was calculated as $\alpha_1+\alpha_2$. Again, this gives an instantaneous recording that does not capture changes over the course of the wingbeat cycle, but facilitates comparison among wingbeat cycles. Note that this estimate does not account for relative air movement resulting from the induced velocity.

Coefficient of lift (C_L): this was estimated based on the overall vertical acceleration of the bat for the entire wingbeat cycle, and the bat's posture and wrist velocity at the time of maximum wingspan, using the equation:

$$C_L = \frac{M_b\left(A_{vert} + \boldsymbol{g}\right)}{\frac{1}{2}\rho V_{wrist}^2 S}, \quad (5)$$

where ρ is the density of air ($1.2\,kg\,m^{-3}$), V_{wrist} is the instantaneous velocity of the wrist in the x_g–z_g plane at the time of maximal wingspan, and wing area (S) is calculated for the same instant in time as V_{wrist}. Calculated this way, C_L is not intended to represent an absolute measure, but rather an assessment of relative aerodynamic effectiveness that can be applied across species and flight speeds.

Statistical analyses

Scaling of body shape

For tests of allometry in body shape parameters, calculations of body shape were made for all 135 flights. Because our species sample size for estimation of scaling relationships was six, we used averages for all individuals within each species. For each parameter, the calculated values from the five trials of an individual were pooled to determine an individual median, then the individual medians within a species were pooled to determine the species median. Those six species medians were used in a log–log orthogonal (reduced major axis or RMA) regression against median body mass for each species (LaBarbera, 1989). To account for statistical non-independence of data resulting from the shared phylogenetic history of the six species (Felsenstein, 1985), we repeated that analysis accounting for phylogeny using a generalized least squares (GLS) model. We used a consensus tree of several recent pteropodid phylogenies (Giannini and Simmons, 2005; Jones et al., 2002; O'Brien et al., 2009), with branch lengths scaled using the method of Pagel (Pagel, 1992). GLM analyses with phylogeny were carried out using REGRESSIONv2 (Lavin et al., 2008) in Matlab. The slope of each regression was compared with that expected under isometry using two-tailed t-tests with four degrees of freedom. For ease of comparison with previous studies, we also present the results of RMA analyses that do not account for phylogeny. The expected relationships under isometry are: $b_{max}\propto M_b^{1/3}$, $b_{min}\propto M_b^{1/3}$, $c_{max}\propto M_b^{1/3}$, $S_{max}\propto M_b^{2/3}$, $Q_s\propto M_b^{1/3}$ and $AR\propto M_b^{0}$ (Norberg, 1990).

Scaling of flight velocity

The speed at which a bat flies is expected to increase with the size of the bat, and that prediction results because wing loading (Q_s) scales $\propto M_b^{1/3}$ under isometry. Rearrangement of Eqns 1 and 5 reveals that as Q_s increases, A_{vert} will decrease, unless there is an associated increase in the product of C_L and V_{wrist}^2:

$$A_{vert} = \boldsymbol{g}\left(\frac{C_L\frac{1}{2}\rho V_{wrist}^2}{Q_s} - 1\right). \quad (6)$$

Assuming that C_L does not increase with body mass, and assuming V_{wrist} is proportional to V_{horiz}, large animals should fly faster than small ones in order to generate the lift required to fly. Specifically, preferred flight velocity is predicted to scale $\propto M_b^{1/6}$ (Pennycuick, 1975).

We expected bats flown in the corridor to fly with speeds that scaled with $M_b^{1/6}$, but since bats in the wind tunnel could not choose their own velocities, we did not expect those individuals to conform to that pattern. We thus performed a linear least squares regression of $\log(V_{horiz})$ *versus* $\log(M_b)$ for the median V_{horiz} values of individuals flown in the corridor (N=22). A GLS model that accounted for phylogenetic effects was used, and the slope of that regression was compared with 1/6 using a two-tailed t-test with eight degrees of freedom. For ease of comparison with previous studies, we also include the slope estimate based on an ordinary RMA regression.

Scaling of wing kinematics

To test for systematic changes in the values of kinematic parameters with body size, we performed linear least squares regressions of individual median values against $\log(M_b)$. Because bats flown in the wind tunnel (*C. brachyotis*) had different velocity distributions than corridor-flown bats (see Results), we excluded them from kinematic scaling analyses.

To account for phylogenetic effects, we performed all interspecific regression analyses using a GLS model, as described above, with reduced degrees of freedom to account for soft polytomies in the pteropodid tree (Purvis and Garland, 1993; Garland and Díaz-Uriarte, 1999). Parameters included in these analyses were T, T_{down}, τ, ϕ, St, β, wing camber, α, α_1, α_2 and C_L.

We expected T and T_{down} to scale with $M_b^{1/3}$ (Norberg, 1990), and all other regressions were expected not to scale with body mass, in other words, were expected to scale $\propto M_b^{0}$.

We used log–log regression for the majority of tests but could not use that method for angles (ϕ, β, α, α_1 and α_2), since many angles were negative (Smith, 1984). Instead, we used log–linear regression for angles, which assumes that if there is an effect of body size on the angle, it scales $\propto M_b^{1}$.

For ease of comparison with previous studies, we repeated linear regressions of kinematic parameters against body mass using more classical RMA methods that do not account for phylogeny.

Changes of kinematics with velocity and acceleration

To determine how wing kinematics change with V_{horiz}, A_{horiz} and A_{vert}, we used multiple regression. This method permits examination of how each of these three variables correlates with changes in wing kinematics, while correcting for the influence of the other two. Each regression had a single kinematic variable as the dependent variable, and V_{horiz}, A_{horiz} and A_{vert} as model effects. To take into account variability among individuals, we also included individual bat as a random effect (Gelman and Hill, 2007). We performed these regressions separately for each species.

We conducted regression analysis for b_{max}, b_{min}, T, T_{down}, τ, ϕ, β, St, α, α_1, α_2, wing camber and C_L. Thus, thirteen multiple regression analyses were performed per species, for a total of 78. In each, we tested for significance of partial regression coefficients for each of V_{horiz}, A_{horiz} and A_{vert} using two-tailed t-tests. Degrees of freedom for each multiple regression test were equal to N–k, where N is the number of flight trials, and k is the number of estimated parameters. Estimated parameters were V_{horiz} partial regression slope, A_{horiz} partial regression slope, A_{vert} partial regression slope, and one intercept per individual bat. This resulted in nine degrees

of freedom for *R. aegyptiacus* regressions, 13 for those of *P. vampyrus*, and 17 degrees of freedom for those of all other species.

Statistical analyses were performed using custom-scripts in Matlab R2008b (MathWorks Inc., Natick, MA, USA), then verified using JMP IN 8.0 (SAS Institute, Cary NC, USA). For models with random effects we used the expected mean squares (EMS) method. To account for possibly inflated family-wise type I error rate resulting from performing multiple statistical tests on closely related data (Curran-Everett, 2000; Curran-Everett and Benos, 2004), we carried out a positive false discovery rate (pFDR) analysis on *P*-values from the data in supplementary material Table S2A–C using the qvalue package (Version 1.20) (Storey, 2002) for R (Version 2.10.1) (R Development Core Team, 2009) with a pFDR rate of 5% (allowing 5% of 'significant' results to be false). From that analysis we found that a more conservative alpha level for significance is 0.034, rather than 0.05, and used the more conservative value as the criterion for rejection of the null hypothesis (supplementary material Table S2A–C).

RESULTS

A complete table of summary statistics for all 135 trials used in this study is provided in supplementary material Table S1. In the body of this paper, we report phylogenetically corrected regression statistics, but for ease of comparison with previous studies, we include results without phylogenetic correction in tables as well.

Scaling of body shape

The scaling of maximum wingspan to body mass was positively allometric ($b_{max} \propto M_b^{0.423}$ compared with $M_b^{0.333}$, P=0.045; Table 2, Fig. 3A). Minimum wingspan scaled isometrically to body mass ($b_{min} \propto M_b^{0.366}$ compared with $M_b^{0.333}$, P=0.509; Table 2, Fig. 3B). Wing chord scaled isometrically with body mass ($c_{max} \propto M_b^{0.357}$ compared with $M_b^{0.333}$, P=0.457; Table 2, Fig. 3C). Wing area scaled with positive allometry ($S_{max} \propto M_b^{0.768}$ compared with $M_b^{0.666}$, P=0.047; Table 2, Fig. 3D) and wing loading increased more gradually with body size than would be expected under isometry ($Q_s \propto M_b^{0.233}$ compared with $M_b^{0.333}$, P=0.024; Table 2, Fig. 3E). Since span increased with positive allometry but chord increased isometrically, aspect ratio increased with M_b, with the slope of that regression approaching significant allometry ($AR \propto M_b^{0.072}$ compared with $M_b^{0.000}$, P=0.068; Table 2, Fig. 3F).

Flight velocities and accelerations

The horizontal velocities of bats (4.98±0.09 m s^{-1}) were much greater than vertical velocities (0.12±0.03 m s^{-1}), so flight paths were close to horizontal (1.36±0.36 deg above horizontal). The flight speeds of bats of all body sizes overlapped greatly. Bats in the wind tunnel (*C. brachyotis*) generally flew faster for their size than bats in the corridor did (Fig. 4A). With wind tunnel flights excluded from analysis, the preferred velocities of animals increased with M_b with a slope not significantly different from that expected under isometry ($V_{horiz} \propto M_b^{0.005}$ compared with $M_b^{0.167}$; P=0.056; Table 3) but much closer to $M_b^{0.000}$ (P=0.948). We found considerable variability in A_{horiz} and A_{vert} among trials (Fig. 4B,C), and no trial showed zero net acceleration.

Scaling of wing kinematics

The regression slope of wingbeat period to body mass was significantly lower than that expected under isometry ($T \propto M_b^{0.180}$ compared with $M_b^{0.333}$; P=0.039; Table 3, Fig. 5A), but downstroke duration was not significantly different from predicted ($T_{down} \propto M_b^{0.213}$ compared with $M_b^{0.333}$, P=0.140; Table 3, Fig. 5B). Downstroke ratio also did not change significantly with body size ($\tau \propto M_b^{0.036}$ compared with $M_b^{0.000}$; P=0.162; Table 3, Fig. 5C).

Wing stroke amplitude at the wrist did not significantly change with log body mass [$\phi \propto (\log M_b) \cdot (-6.058)$; P=0.257; Table 3, Fig. 5D], nor did stroke plane angle [$\beta \propto (\log M_b) 8.974$; P=0.107; Fig. 5E]. Strouhal number also did not change significantly with log body mass ($St \propto M_b^{-0.088}$ compared with $M_b^{0.000}$; P=0.532; Table 3, Fig. 5F).

We found that α increased significantly with log body mass [$\alpha \propto (\log M_b) 7.738$; P=0.014; Table 3, Fig. 5G], and that the overall

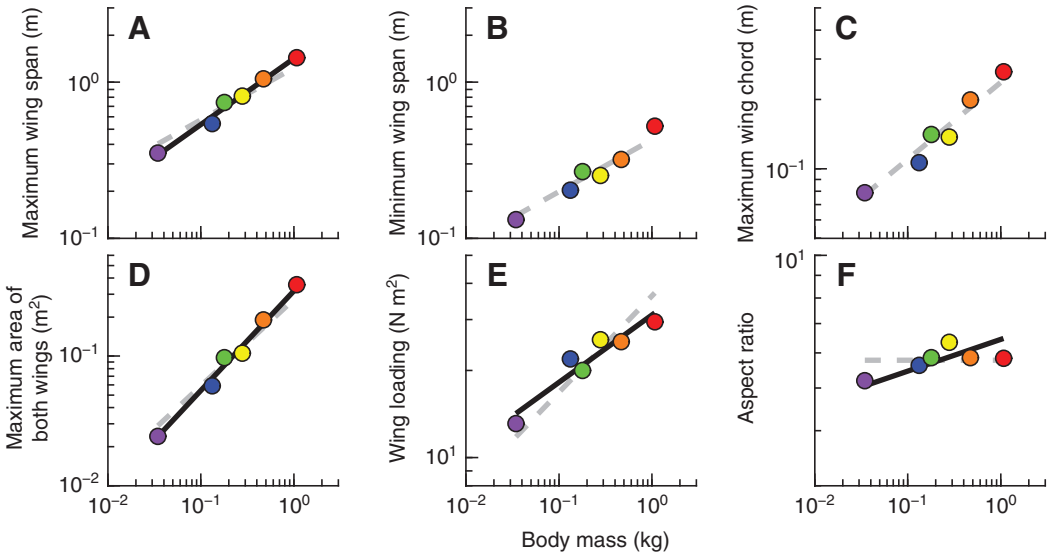

Fig. 3. Log–log phylogenetic GLS RMA regressions of wing shape parameters against body mass after phylogenetic correction. Circles represent medians for each species. Expected slopes under isometry are denoted by the grey dashed line. Where data approached or achieved statistically significant allometry, the best fit line is shown in black. (A) Maximum wingspan, (B) minimum wingspan, (C) wing chord, (D) maximum wing area, (E) wing loading, and (F) aspect ratio. Slope estimates are reported in Table 2.

Table 2. Results from regression analyses of several body shape variables against M_b

		Reduced major axis regression (non-phylogenetic)				Generalized least squares (phylogenetic)		
	Isometry slope	Previously published dead specimen study slopes	Slope estimate ± standard error, (95% C.I.)	*t*-statistic, d.f.	Two-tailed *P*	Slope estimate	*t*-statistic, d.f.	Two-tailed *P*
Maximum wingspan (b_{max})	$\propto M_b^{0.333}$	0.350[a]; 0.362±0.050[b]	0.422±0.026 (0.350 0.494)	3.438, 4	0.026*	0.423	2.886, 4	0.045*
Minimum wingspan (b_{min})	$\propto M_b^{0.333}$	–	0.391±0.039 (0.283 0.499)	1.501, 4	0.208	0.366	0.724, 4	0.509
Maximum wing chord (c_{max})	$\propto M_b^{0.333}$	–	0.368±0.039 (0.260 0.476)	0.897, 4	0.420	0.357	0.822, 4	0.457
Maximum wing area (S_{max})	$\propto M_b^{0.666}$	0.715[a]; 0.691±0.099[b]	0.795±0.045 (0.670 0.920)	2.844, 4	0.047*	0.768	2.845, 4	0.047*
Wing loading (Q_s)	$\propto M_b^{0.333}$	0.327[a]; 0.309±0.092[b]	0.242±0.037 (0.139 0.345)	2.435, 4	0.072	0.233	3.524, 4	0.024*
Aspect ratio (AR)	$\propto M_b^{0}$	0.110[a]; 0.033±0.058[b]	0.056±0.021 (–0.002 0.114)	2.705, 4	0.054	0.072	2.481, 4	0.068

Dead specimen study slopes are regression coefficients from two scaling studies of pteropodid bats ([a]Norberg and Rayner 1987; [b]Norberg, 1981). Slopes that differ significantly from isometry are labeled with asterisks (*P<0.05, **P<0.01).

change occurred as a result of changes in α_1 but not α_2 [$\alpha_1 \propto (\log M_b) 7.542$; P=0.032; Fig. 5H; and $\alpha_2 \propto (\log M_b) \cdot (-0.461)$; P=0.866; Table 3, Fig. 5I]. Wing camber at maximum span did not change significantly with log body mass (wing camber$\propto M_b^{0.070}$; P=0.714; Fig. 5J). Coefficient of lift increased significantly with body mass ($C_L \propto M_b^{0.170}$; P=0.042; Table 3, Fig. 5K).

Kinematic changes with velocity and acceleration

We observed several changes in the kinematics of bats with changes in V_{horiz}, A_{horiz} and A_{vert}. Some changes that were significant in some species were not significant in others, but in almost no cases did different species show opposing trends; where a partial regression slope was significant for multiple species, it almost always had the same sign, positive or negative, for all other species. These are reported fully in supplementary material Table S2, and summarized in Table 4.

With increases in flight velocity, holding the influences of A_{horiz} and A_{vert} constant, we observed decreased maximum wingspan, increased wingbeat period, increased downstroke duration, increased downstroke ratio, decreased stroke plane angle, decreased angle of attack, decreased wing camber, decreased Strouhal number, and decreased lift coefficient. We observed no significant change in amplitude, and observed mixed results among species for changes in minimum wingspan (Table 4, supplementary material Table S2A).

With increases in horizontal acceleration, we observed decreases in minimum wingspan and stroke plane angle, and increases in maximum wingspan, amplitude and angle of attack. Strouhal number and lift coefficient also both increased. We saw no significant changes in wingbeat period, downstroke duration, downstroke ratio or wing camber (Table 4, supplementary material Table S2B).

With increases in vertical acceleration, we observed an increase in maximum wingspan, angle of attack, wing camber, Strouhal number and lift coefficient, along with a decrease in wingbeat period. We observed no significant changes in minimum wingspan, downstroke duration, downstroke ratio, wing stroke amplitude, or stroke plane angle (Table 4, supplementary material Table S2C).

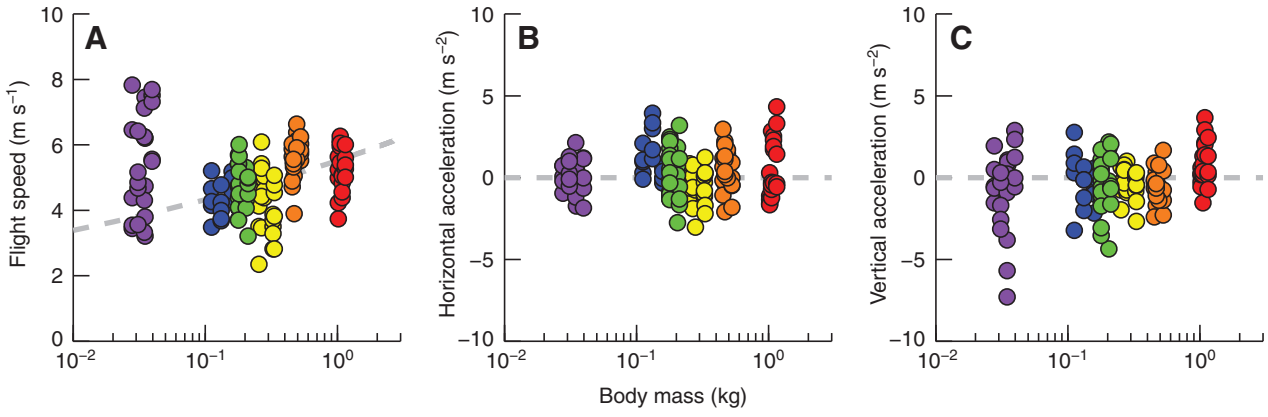

Fig. 4. Velocities and accelerations for the 135 wingbeat cycles in this study. The smallest bats (*C. brachyotis*; purple) were flown in a wind tunnel whereas other bats were flown in a flight corridor. (A) For corridor-flown bats, velocity increased with body mass as expected under isometry ($V_{horiz} \propto M_b^{1/6}$; dashed grey line), but bats flown in the wind tunnel usually flew faster than would be predicted based upon extrapolation of that line to their range of masses. (B,C) The magnitudes of A_{horiz} (B) and A_{vert} (C) were centered close to zero, but no trial showed zero net acceleration.

Table 3. Results from regression analyses of several kinematic variables against M_b

		Ordinary least squares (non-phylogenetic)			Generalized linear model (phylogenetic)		
	Isometry slope	Slope estimate ± s.e.m. (95% C.I.)	*t*-statistic, d.f.	Two-tailed *P*	Slope estimate ± s.e.m. (95% C.I.)	*t*-statistic, d.f.	Two-tailed *P*
Horizontal speed (V_{horiz})	$\propto M_b^{0.167}$	0.106±0.040 (0.023 0.189)	–1.515, 20	0.146	0.005±0.072 (–0.161 0.171)	–2.234, 8	0.056
Wingbeat period (T)	$\propto M_b^{0.333}$	0.303±0.043 (0.213 0.393)	–0.697, 20	0.494	0.180±0.062 (0.037 0.323)	–2.459, 8	0.039*
Downstroke duration (T_{down})	$\propto M_b^{0.333}$	0.353±0.055 (0.238 0.468)	0.350, 20	0.730	0.213±0.074 (0.042 0.384)	–1.637, 8	0.140
Downstroke ratio (τ)	$\propto M_b^{0}$	0.045±0.015 (0.014 0.076)	3.035, 20	0.007**	0.036±0.023 (–0.017 0.089)	1.542, 8	0.162
Wing stroke amplitude (ϕ)	$\propto$(log M_b) 0	–0.011±3.117 (–6.513 6.491)	–0.003, 20	0.997	–6.058±4.961 (–17.498 5.382)	–1.221, 8	0.257
Stroke plane angle (β)	$\propto$(log M_b) 0	3.847±3.399 (–3.243 10.937)	1.132, 20	0.271	8.974±4.939 (–2.415 20.363)	1.817, 8	0.107
Strouhal number (St)	$\propto M_b^{0}$	–0.018±0.065 (–0.154 0.118)	–0.275, 20	0.786	0.088±0.134 (–0.221 0.397)	0.653, 8	0.532
Angle of attack (α)	$\propto$(log M_b) 0	4.450±1.451 (1.423 7.477)	3.067, 20	0.006**	7.738±2.477 (2.026 13.45)	3.124, 8	0.014*
α_1	$\propto$(log M_b) 0	5.682±2.060 (1.385 9.979)	2.759, 20	0.012*	7.542±2.903 (0.848 14.236)	2.598, 8	0.032*
α_2	$\propto$(log M_b) 0	0.751±1.457 (–2.288 3.790)	0.516, 20	0.612	–0.461±2.648 (–6.567 5.645)	–0.174, 8	0.866
Wing camber	$\propto M_b^{0}$	–0.057±0.106 (–0.278 0.164)	–0.536, 20	0.598	0.070±0.184 (–0.354 0.494)	0.379, 8	0.714
Lift coefficient (C_L)	$\propto M_b^{0}$	0.051±0.042 (–0.037 0.139)	1.196, 20	0.246	0.170±0.070 (0.009 0.331)	2.411, 8	0.042*

Log–log regressions were performed for most variables, but log–linear regressions were performed for angular data (ϕ, β, α, α_1 and α_2), since they frequently included negative numbers which cannot be log-transformed. Slopes that differ significantly from isometry are labeled with asterisks (*P<0.05, **P<0.01).

DISCUSSION

The influence of body size on wing shape and kinematics

Our results provide experimental evidence that for pteropodid bats many aspects of wing kinematics vary with body size, but that the ways kinematics change with velocity and acceleration are relatively consistent across body sizes. Additionally, we found that the scaling relationships for maximum wingspan, maximum wing area and minimum wing loading in pteropodid bats, based on measurements from actual wing form as employed during flight behavior, differ from the scaling relationships measured from outstretched preserved specimens (Table 2). Importantly, we uncovered a significant positive allometry between body mass and wing area during the downstroke, which may help to offset the consequences of higher wing loading that accompany increased body size. Furthermore, large bats had higher coefficients of lift during flight than small bats did. This result highlights the importance of wing posture as a confounding variable for hypotheses about ecological function based solely on the two-dimensional shape of an outstretched wing.

Body size and wing shape: the importance of posture

A bat's wing comprises highly compliant skin membranes that interconnect a jointed skeleton capable of many degrees of freedom

Table 4. Summary table showing the kinematic correlates of changes in one of V_{horiz}, A_{horiz} or A_{vert}, with the influence of the other two held constant

	With increasing V_{horiz}						With increasing A_{horiz}						With increasing A_{vert}					
	Cb	*Ra*	*Pp*	*Eh*	*Ph*	*Pv*	*Cb*	*Ra*	*Pp*	*Eh*	*Ph*	*Pv*	*Cb*	*Ra*	*Pp*	*Eh*	*Ph*	*Pv*
Maximum wingspan (b_{max})	–						+				+		+				+	
Minimum wingspan (b_{min})	–			+		+			–									
Wingbeat period (T)			+	+	+									–				
Downstroke duration (T_{down})			+	+	+													
Downstroke ratio (τ)			+		+													
Wing stroke amplitude (ϕ)									+									
Stroke plane angle (β)	–	–	–	–	–		–	–	–	–								
Angle of attack (α)	–		–			–					+		+					
α_1	–		–				–		–	–						–		
α_2					–	–	+	+	+	+	+	+						+
Wing camber	–	–		–	–												+	
Strouhal number (St)	–	–	–	–	–	–	+		+	+						+		
Lift coefficient (C_L)	–	–	–	–	–							+	+	+	+		+	+

A '+' or '–' symbol is shown where the partial regression slope for a species is significantly positive or negative (P<0.034), respectively.
Species abbreviations are defined in Table 1. The trend of + and – symbols appearing together only one time out of 39 suggests that the kinematic mechanisms by which bats modulate speed, thrust and lift are similar across body sizes.

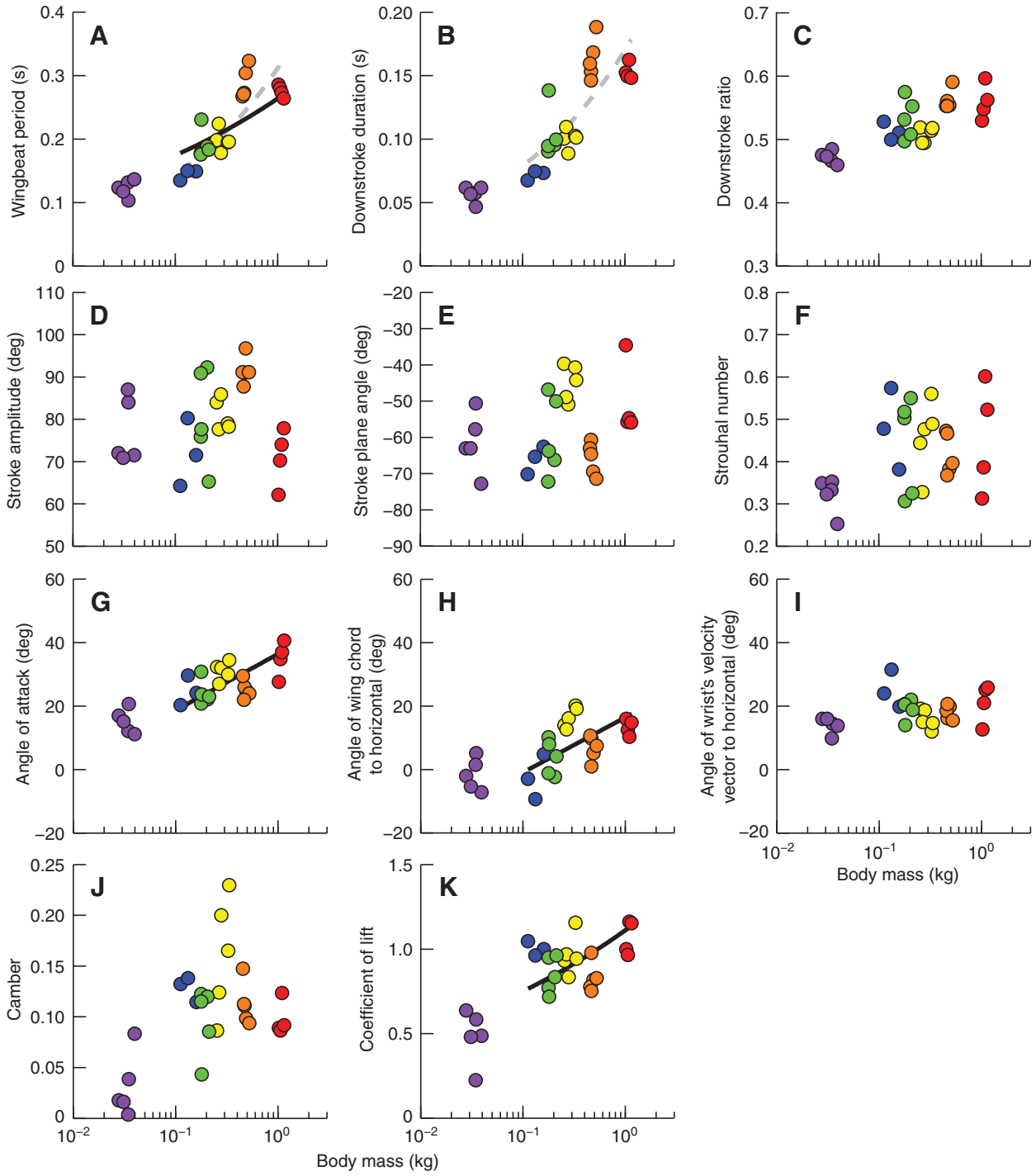

Fig. 5. Median kinematic parameter values *versus* log body mass for the 27 bats in this study. Regression slopes were calculated after phylogenetic correction (Table 3), and excluded *C. brachyotis* because they were flown in a wind tunnel. Wingbeat period (A) scaled lower than expected under isometry. Downstroke duration (B), Downstroke ratio (C), stroke amplitude (D), stroke plane angle (E) and Strouhal number (F) did not change significantly with body mass. Angle of attack increased with body size (G) as a result of a change in α_1 (H), but not from a change in α_2 (I). Wing camber (J) did not change with body size, but coefficient of lift (K) did.

(Riskin et al., 2008). By its very morphological structure, the area of a bat wing is highly variable throughout every wingbeat cycle. As a result, measurements of wing area for bat specimens can vary substantially compared with those for insects or birds, depending especially on the degree to which the membrane is stretched before preservation or measurement. It has been extremely valuable to make comparisons of wing area among bat species in a two-dimensional perspective, but our high-fidelity measurements of wing shape permitted the use of actual three-dimensional wing conformation in flight.

It has long been known that the bodies of pteropodid bats do not scale isometrically (Norberg, 1981; Norberg, 1990; Norberg and Rayner, 1987), but several scaling relationships that we observed in this study differ from those previously reported based on

measurements of dead specimens measured outstretched on a flat surface. We hypothesize that those discrepancies arise because wing posture during the downstroke does not match the posture in which bats are typically held for morphometric measurements, and the difference between in-flight conformation and measurement conformation varies non-randomly with body size. In other words, we hypothesize that the way bats position their wings during downstroke varies with body size. If true, the actual scaling trends in the mid-flight shapes of bat wings would present themselves only when wing measurements were taken during flight. Given that wing measurements are widely used to predict behavior and foraging ecology for bat species (e.g. Bullen and McKenzie, 2001; Kingston et al., 2000), our hypothesis, if true, would have wide-reaching influence on our understanding of bat evolution and ecology.

In their analysis of wing form in bats, Norberg and Rayner (Norberg and Rayner, 1987) and Norberg (Norberg, 1981) found that wingspan in pteropodids scaled with $M_b^{0.350}$ and $M_b^{0.362}$, respectively, both only slightly higher than the $M_b^{0.333}$ expected under isometry. The scaling relationship uncovered in this study ($b_{max} \propto M_b^{0.423}$) was around 20% higher than theirs and suggests that large bats extend the wing membrane more fully during the downstroke than small bats do. Similarly, the scaling coefficient of wing loading to body mass from this study, $Q_s \propto M_b^{0.233}$, was around 27% lower than the coefficients $M_b^{0.327}$ and $M_b^{0.309}$ reported by Norberg and Rayner (Norberg and Rayner, 1987) and Norberg (Norberg, 1981). Here again, posture is a probable contributor to the discrepancy. The area of a bat's wing changes throughout the wingbeat cycle and depends greatly on the positions of the carpus and elbow and the degree of extension and abduction of the digits. Whereas specimens in previous studies have been measured in a fully outstretched and flattened posture, our methods capture the three-dimensional shape of the wing with the degree of wing extension that is biologically relevant.

Interestingly, our results suggest that large bats extend the wing more fully on the downstroke, but not on the upstroke, since the scaling relationship of b_{min} to body mass ($b_{min} \propto M_b^{0.366}$) did not differ from the relationship expected under isometry ($b_{min} \propto M_b^{0.333}$). This makes sense, since the majority of lift production occurs on the downstroke.

Since wing loading increases with body mass, it is hypothesized to limit the body sizes of the largest flying animals (Greenewalt, 1975). Norberg (Norberg, 1981) and Norberg and Rayner (Norberg and Rayner, 1987) found that wing loading for pteropodid bats scaled isometrically with body mass ($Q_s \propto M_b^{0.333}$), but we found evidence for negative allometry ($Q_s \propto M_b^{0.233}$). Our result suggests that the largest bats may effectively reduce wing loading, compensating for their large size, by employing different wing postures than small bats. In his study of allometric scaling of bird wings, Nudds commented on the possible influence of body-size-dependent variation in elbow angle among birds on scaling relationships (Nudds, 2007). Whether or not the relationship we report here for pteropodid bats is also true for birds, or indeed even other bats, is an important topic for future study.

An alternative explanation for the difference between our body size regression slopes and those of Norberg and Rayner is that because we sampled fewer species, six in this study compared with >50 by Norberg and Rayner, we simply got different slopes by chance. To assess the influence of sample bias, we performed orthogonal regressions of $\log(M_b)$ *versus* $\log(b_{max})$ and $\log(M_b)$ *versus* $\log(S_{max})$ using Norberg and Rayner's data for the closest species with complete measurements to the six used in this experiment: *Cynopterus brachyotis* (0.0265 kg), *Rousettus aegyptiacus* (0.140 kg), *Pteropus* sp. (0.210 kg), *Eidolon helvum* (0.274 kg), *Pteropus* sp. (0.347 kg) and *Pteropus vampyrus* (1.179 kg). Using Norberg and Rayner's data, we obtained regression slopes of $b_{max} \propto M_b^{0.331\pm0.05}$ and $S_{max} \propto M_b^{0.651\pm0.109}$. Both of those are closer to the regression slopes of Norberg and Rayner's entire pteropodid dataset ($b_{max} \propto M_b^{0.350}$ and $S_{max} \propto M_b^{0.715}$) than to our regression slopes ($b_{max} \propto M_b^{0.423}$ and $S_{max} \propto M_b^{0.768}$). This supports our hypothesis that the difference between their results and ours is our use of mid-flight wing shape measurements, and not the species sample used. Further investigations of species-specific differences in posture will help elucidate the aerodynamic relevance of those differences.

Body size and wing kinematics

Our data suggest that certain information about flight kinematics for any pteropodid species can be assumed to be representative for the group, despite the remarkable range in body sizes in the family. For the kinematic parameters we report here, wing kinematics were similar across the bats surveyed in this study despite more than a 40-fold range in body mass among individuals. Downstroke period scaled as predicted under isometric scaling, and several kinematic variables showed no significant change with body size (τ, ϕ, β, *St*, α_2, wing camber). However, a few variables did change with increasing body size, namely *T*, α and C_L.

Although we found that the relationship between V_{horiz} and M_b did not differ significantly from expected, there was no significant increase in V_{horiz} with M_b. Thus, without air moving faster across the wings, the higher wing loading values of large bats should have required them to have higher lift coefficients than small bats did, and this is what we observed. The higher C_L values of large bats were most likely achieved by their higher wingbeat frequencies (for their size) and their higher angles of attack, since no other variables changed across body sizes. Importantly, the departure from isometry in S_{max} did not contribute to this trend, since the C_L equation (Eqn 5) accounts for wing area.

Strouhal number can be employed as a dimensionless descriptor of flight speed for flapping swimmers and fliers. Regardless of body size, when animals fly with Strouhal numbers between 0.2 and 0.4, propulsive efficiency is thought to be particularly high (Taylor et al., 2003). The Strouhal numbers of corridor-flown animals in this study were around 0.3 to 0.6, slightly higher than the predicted range, but they did not differ significantly with size. Strouhal numbers for pteropodid bats were published previously by Taylor et al. (Taylor et al., 2003) based on data from Bullen and McKenzie (Bullen and McKenzie, 2002), who used two corridor-flown pteropodid species with body masses within the range we investigated here (*Pteropus poliocephalus*: 0.7 kg, and *P. scapulatus* 0.4 kg). Their values were around 0.42, roughly the middle of our range for corridor-flown bats.

Bats flown in the wind tunnel had lower Strouhal numbers than corridor-flown bats did, probably as a result of their relatively high flight velocities. After all, every species decreased *St* with increases in flight speed (Table 4). Interestingly, the Strouhal numbers of wind-tunnel-flown bats fell exactly within the expected 0.2 to 0.4 range. This suggests that when bats fly at high speed they do not adjust their amplitude and frequency to maintain consistent Strouhal numbers. We hypothesize that because we used a wind tunnel to collect data for *C. brachyotis*, we artificially decreased Strouhal number. Conversely, Tobalske et al. (Tobalske et al., 1997) found that the wingbeat frequencies of birds in their study were higher at a given speed in the wind tunnel compared with in the wild, which would increase Strouhal number. Similarly, Liechti and Bruderer found that wind-tunnel flown birds showed higher wingbeat

frequencies than those observed in the wild (Liechti and Bruderer, 2002). Clearly a survey of Strouhal number across taxa that takes experimental conditions into account would be informative.

Changes in wing kinematics with velocity and acceleration

The results from our regression analyses varied across species, but a noteworthy trend emerged: when the partial regression coefficient between some variable and one of the regression effects was significantly different from zero for any species, other species with significant regression slopes almost always showed the same directional trend (Table 4). For example, not all bats had significant changes in wingbeat period with V_{horiz}, but where a significant trend existed, it was always positive. This consistency is remarkable considering that we investigated 13 variables with respect to each of V_{horiz}, A_{horiz} and A_{vert} for a total of 39 regressions per species, and found non-conflicting results from all six species in every case but one (b_{min} *vs* V_{horiz}). The stability of our results suggests that across a broad range of body sizes, bats modify their kinematics similarly with changes in velocity and acceleration.

Kinematic changes with flight velocity

Several previous studies of bat flight have considered the kinematic changes that correlate with differences in flight velocity for bats flying at steady speeds (e.g. Aldridge, 1986; Aldridge, 1987; Lindhe Norberg and Winter, 2006). As V_{horiz} increases, drag increases so that more thrust is required, and air velocity over the wing is increased, enhancing lift. Thus, changes in wing kinematics with increased V_{horiz} might be related to increased thrust production, to drag reduction, to C_L alleviation, or to some combination of those (Hedrick et al., 2002; Tobalske et al., 2007).

Strouhal number, by definition, is inversely proportional to velocity (Eqn 4), so it is not surprising that Strouhal number decreased with increasing V_{horiz}. Similarly, the mid-downstroke velocity of the wrist, correlated with flight velocity, appears in the denominator of the equation for coefficient of lift (Eqn 5), and we see the expected trend of decreased C_L with increased V_{horiz}. In essence, a bat flying quickly has a greater airspeed across the wings than it does flying slowly, and since it weighs the same under those two circumstances, the coefficient of lift must decrease with speed.

All species showed a decrease in stroke plane angle with increased flight velocity, as has been reported for other bat species previously (Aldridge, 1987). Although the wake patterns generated by bats are complex (Hedenström et al., 2007; Hubel et al., 2009), simple models such as actuator disk theory can capture some of the relevant connection between kinematics and aerodynamic force production. According to these ideas, a decrease in stroke plane angle should direct the induced velocity of the wing motion more rearward, thereby shifting the contribution of induced velocity towards increased thrust and away from lift generation, to simultaneously overcome increased drag and diminish the lift production of the wings (Pennycuick, 1975). This explanation has been applied to changes in stroke plane angle with speed in previous studies (Norberg, 1990; Pennycuick, 1975), and fits our results as well.

Bats showed a trend toward longer wingbeat cycle with increased velocity, and the downstroke phase of the wingbeat cycle was particularly long. Amplitude, however, did not change with speed. This differs from the trends reported for birds, in which wingbeat period increases with speed because of changes in the duration of upstroke, and amplitude does not change (Hedrick et al., 2002; Hedrick et al., 2003). The lengthening of the downstroke by bats may contribute to the reduction in C_L that we observed by slowing the downward motion of the wings during downstroke. Angle of attack and wing camber also both decreased with increased flight velocity, and those trends would also both reduce lift.

Only *C. brachyotis* showed a significant decrease in both maximum and minimum wingspan with increases in flight velocity. We hypothesize that this resulted because *C. brachyotis* were flown in a wind tunnel, and therefore flew at higher velocities relative to their body sizes than did the corridor-flown bats. Since drag increases exponentially with velocity, *C. brachyotis* probably encountered relatively larger drag forces than did the other bats. We hypothesize that *C. brachyotis* decreased overall wingspan with increasing flight velocity to reduce drag and that the difference between *C. brachyotis* and other species reflects this. We hypothesize that reduction of maximum wingspan with flight speed only occurs for bats at high flight speeds. We predict that maximum wingspan would not change with V_{horiz} below some threshold speed for *C. brachyotis*, and that other bat species would show a negative correlation between wingspan and flight speed at high speeds.

Horizontal accelerations: thrust production and drag reduction

Over the course of a wingbeat cycle, the orientations of aerodynamic thrust, drag and lift change relative to global axes and can vary along the span of the flapping wing (Norberg, 1976). However, if we consider only the summation of forces over the whole wingbeat cycle, and if we neglect deviations from horizontal flight, we can treat horizontally directed net force as the sum of thrust and drag, and vertically directed net force as lift. This approach simplifies comparisons among individuals and flight conditions, and we employ that simplification here.

The net A_{horiz} of a flying bat results from the sum of forward thrust and rearward drag over the course of the entire wingbeat cycle, and the relative contributions of each over time cannot be separated in a purely kinematic analysis (Hedrick et al., 2002). Thus, the kinematic correlates of increased A_{horiz} might increase thrust, decrease drag, or do both. Still other changes might not influence those aerodynamic forces directly but change as a secondary result of kinematic changes that do.

When bats increased A_{horiz}, their stroke plane angles became more negative, thereby making the path of the wingtip more vertical. We hypothesize that a more vertical wing path shifts the orientation of shed vortices rearward, thereby increasing thrust (Pennycuick, 1975). With increases in A_{horiz} some species also increased wingspan, which would reduce the magnitude of induced drag slightly and might also increase thrust by sweeping the wings through a greater volume of air.

Strouhal number increased with A_{horiz}, probably as a secondary result of the decreased stroke plane angle; because stroke plane angle became more vertical while amplitude either increased or did not change, the maximum vertical distance traveled by the wingtip increased, and thus so did Strouhal number.

Angle of attack did not change significantly with A_{horiz} for most species, but its component angles, α_1 and α_2, did. All species showed decreases in α_2 with increasing A_{horiz}, probably also because of the decreased stroke plane angle. Since wingbeat frequency did not change with A_{horiz}, the decrease in stroke plane angle caused the leading edge of the wing to move more vertically during downstroke relative to the oncoming flow, resulting in an increase in α_2 for all species. That increase alone would have increased the angle of attack, but the overall angle of attack did not increase with A_{horiz} for any species except *P. hypomelanus*. This occurred because all species except *P. hypomelanus* compensated for the increased α_2 by holding the wing in a more horizontal plane during downstroke,

that is, decreasing α_1. The decrease in α_1 with A_{horiz} was significant for three species, and nearly significant for two ($P<0.07$). We hypothesize that as the result of those kinematic changes, bats were able to take advantage of the added thrust that resulted from a decreased stroke plane angle without suffering the drag-inducing effects of an increased angle of attack.

A few species showed trends with increases in A_{horiz} not seen in other species. *Pteropus pumilus* increased wing stroke amplitude with A_{horiz}, *P. hypomelanus* decreased the downstroke ratio and increased angle of attack, and *P. vampyrus* increased its lift coefficient. No bats showed significant changes in wingbeat period, downstroke duration, or wing camber.

Vertical accelerations: lift production

Vertical acceleration results from increased lift, so the kinematic correlates of A_{horiz} should cause increased lift, or result from correlations to kinematic changes that do so. Many kinematic parameters, such as T_{down}, τ, ϕ and β, did not change significantly with increased lift production, even though aerodynamic theory would suggest that many of those variables could influence lift if modified (Norberg, 1990). Bat species typically increased lift production by flapping their wings more quickly (decreasing T), though the duration of the downstroke was not correlated with lift production for any species. Bats also increased lift by increasing wingspan and wing camber. Angle of attack increased with lift production for most species, but that trend was only significant for *C. brachyotis*. Not surprisingly, the lift coefficient, computed with A_{vert} in the numerator (Eqn 5), was positively correlated with A_{vert}.

Wind tunnel *versus* corridor flights

Wind tunnels provide substantial benefits for scientific investigations over the use of animals in free flight, including that the investigator can control the speed at which the animal carries out locomotion, and can collect data for a considerable period of time without need to move equipment alongside a free-moving animal. However, wind tunnels might induce kinematics that would not otherwise occur. For example, Tobalske et al. and Liechti and Bruderer found that birds flown in a wind tunnel had higher wingbeat frequencies than birds of the same species did in the wild (Liechti and Bruderer, 2002; Tobalske et al., 1997). Similarly, we believe that a number of differences between *C. brachyotis* and the other species used in this study probably resulted from the use of a wind tunnel for that species. Specifically, *C. brachyotis* flown in the wind tunnel flew at generally higher velocities and lower Strouhal numbers than would be predicted based on the size–velocity relationship uncovered for corridor-flown bats (Fig. 4A, Fig. 5F). This speed difference probably underlies all other kinematic differences between *C. brachyotis* and the trends we saw in the corridor-flown bats.

If the best fit lines for the five corridor-flown species are used to predict what *C. brachyotis* would have done if flown in a corridor, we see that wingbeat period was higher than expected (Fig. 5A), α_2 slightly lower than expected (Fig. 5I), and wing camber and coefficient of lift were lower than those of other species (Fig. 5J,K). Interestingly, all of these trends are what would be expected for high-speed flight based on our regression analyses (Table 4). With increasing V_{horiz}, bats increased wingbeat period and decreased wing camber and coefficient of lift. Also, when bats increased thrust production to increase A_{horiz}, they increased α_2, and it is likely that for fast flight, such as that of *C. brachyotis* in a wind-tunnel, the relatively higher drag necessitated increased thrust. Obviously, complete resolution of flight speed and the use of a wind tunnel on wing kinematics requires detailed investigation of individual bats flown in a corridor and wind tunnel over a comparable range of speeds, but our results provide an intriguing view of biases that may be introduced by wind tunnel experiments in studies of aerial locomotion.

Implications for non-pteropodid bats

Many of the trends reported here are consistent with patterns observed previously for other bats, but the data in this study might not be representative for bats of all species. Most bats are insectivorous, and many require high levels of maneuverability to catch their evasive food in flight. By contrast, all six species in this study are frugivorous bats that fly nightly between their roosts and food resources and this was probably also true of their last common ancestor (Boon and Corlett, 1989; DeFrees and Wilson, 1988; Jones and Kunz, 2000; Kunz and Jones, 2000; Kwiecinski and Griffiths, 1999; Luft et al., 2003; Giannini and Simmons, 2005; Jones et al., 2002; Teeling et al., 2005). To determine whether bats with improved maneuverability show different kinematic trends with speed and acceleration to those reported here is an exciting objective for future investigations.

Finally, no other family of bats approaches the largest body sizes of pteropodids, and there is a tremendous diversity of bats below the 33 g body mass of our smallest individuals. Small bats tend to fly at lower speeds than the bats in this study did (Akins et al., 2007), suggesting that the $V_{horiz} \propto M_b^{1/6}$ trend reported here might be more robust among bats with smaller body sizes than we observed here. Recent work has revealed that small bats generate leading-edge vortices while flying at low speeds, much like flapping insects do (Muijres et al., 2008), and parallel experiments have not yet been performed for larger bats. Thus, the aeromechanics of bats may differ across the lower spectrum of bat body sizes. Our results demonstrate remarkable consistency in flight mechanics for medium to large-sized bats, and we look forward to parallel studies of smaller bats, especially from non-pteropodid families, that test the applicability of our results to bats in general.

ACKNOWLEDGEMENTS

We thank Allyce Sullivan, Pere Tiemo, and Sarah Taylor for assistance in data collection, and thank the many undergraduates at Brown University who assisted in digitizing the movies for this project. We thank Yvonne Dzal, Ty Hedrick, David Lee, David Lentink, Crystal Linkletter, members of the Swartz and Breuer lab groups, members of the Morph Group at Brown University, and two anonymous reviewers for helpful discussions around this project. We also thank Allyson Walsh and the Lubee Bat Conservancy for access to bats and facilities for data collection. This study was supported by the United States Air Force Office of Scientific Research (AFOSR) and the National Science Foundation (NSF).

LIST OF SYMBOLS AND ABBREVIATIONS

A_{horiz}	net forward acceleration for the wingbeat cycle ($m\,s^{-2}$)
AR	aspect ratio (dimensionless)
A_{vert}	net vertical acceleration for the wingbeat cycle ($m\,s^{-2}$)
b_{max}	maximum wingspan (m)
b_{min}	minimum wingspan (m)
C_L	coefficient of lift (dimensionless)
c_{max}	maximum wing chord (m)
COM	center of mass
d.f.	degrees of freedom
DLT	direct linear transformation
$\boldsymbol{g}$	acceleration of gravity ($9.81\,m\,s^{-2}$)
GLM	generalized linear model
M_b	body mass (kg)
Q_s	wing loading ($N\,m^{-2}$)
RMA	reduced major axis
S	wing area (m^2)
S_{max}	maximum wing area (m^2)
St	Strouhal number
T	wingbeat period (s)

T_{down}	downstroke duration (s)
V_{horiz}	forward velocity ($m\,s^{-1}$)
V_{vert}	vertical velocity ($m\,s^{-1}$)
V_{wrist}	velocity of the wrist in the x_g–z_g plane at the time of max wingspan ($m\,s^{-1}$)
x_b	body-centered x dimension
x_g	global x dimension
y_b	body-centered y dimension
y_g	global y dimension
z_b	body-centered z dimension
z_g	global z dimension
α	angle of attack at mid-downstroke (deg; $\alpha=\alpha_1+\alpha_2$)
α_1	angle of wing chord to horizontal at mid-downstroke (deg)
α_2	angle of wrist trajectory to oncoming flow at mid-downstroke (deg)
β	stroke plane angle (deg)
ρ	density of air ($1.204\,kg\,m^{-3}$)
τ	downstroke ratio (dimensionless)
ϕ	stroke amplitude (deg)

REFERENCES

Abdel-Aziz, Y. I. and Karara, H. M. (1971). Direct linear transformation from comparator coordinates into object space coordinates in close-range photogrammetry. In *Proceedings of the Symposium on Close-Range Photogrammetry*, pp. 1-18. Falls Church, VA: American Society of Photogrammetry.

Akins, J. B., Kennedy, M. L., Schnell, G. D., Sánchez-Hernández, C., Romero-Almaraz, M. De L., Wooten, M. C. and Best. T. L. (2007). Flight speeds of three species of Neotropical bats: *Glossophaga soricina*, *Natalus stramineus*, and *Carollia subrufa*. *Acta Chiropterol.* **9**, 477-482.

Aldridge, H. D. J. N. (1986). Kinematics and aerodynamics of the greater horseshoe bat, *Rhinolophus ferrumequinum*, in horizontal flight at various speeds. *J. Exp. Biol.* **126**, 479-497.

Aldridge, H. D. J. N. (1987). Body accelerations during the wingbeat in six bat species: the function of the upstroke in thrust generation. *J. Exp. Biol.* **130**, 275-293.

Biewener, A. A. (1983). Allometry of quadrupedal locomotion: the scaling of duty factor, bone curvature and limb orientation to body size. *J. Exp. Biol.* **105**, 147-171.

Biewener, A. A. (2005). Biomechanical consequences of scaling. *J. Exp. Biol.* **208**, 1665-1676.

Boon, P. P. and Corlett, R. T. (1989). Seed dispersal by the lesser short-nosed fruit bat (*Cynopterus brachyotis*, Pteropodidae, Megachiroptera). *Malay. Nat. J.* **42**, 251-256.

Brown, J. H. and West, G. B. (2000). *Scaling in Biology*. Oxford: Oxford University Press.

Bullen, R. D. and McKenzie, N. L. (2001). Bat airframe design: flight performance, stability and control in relation to foraging ecology. *Aust. J. Zool.* **49**, 235-261.

Bullen, R. D. and McKenzie, N. L. (2002). Scaling bat wing beat frequency and amplitude. *J. Exp. Biol.* **205**, 2615-2626.

Combes, S. A. and Daniel, T. L. (2003). Into thin air: contributions of aerodynamic and inertial-elastic forces to wing bending in the hawkmoth *Manduca sexta*. *J. Exp. Biol.* **206**, 2999-3006.

Curran-Everett, D. (2000). Multiple comparison: philosophies and illustrations. *Am. J. Physiol. Reg. Integr. Comp. Physiol.* **279**, R1-R8.

Curran-Everett, D. and Benos, D. J. (2004). Guidelines for reporting statistics in journals published by the American Physiological Society. *J. Appl. Physiol.* **97**, 457-459.

DeFrees, S. L. and Wilson, D. E. (1988). *Eidolon helvum*. *Mamm. Sp.* **312**, 1-5.

Dial, K. P. and Biewener, A. A. (1993). Pectoralis muscle force and power output during different modes of flight in pigeons (*Columba livia*). *J. Exp. Biol.* **176**, 31-54.

Dial, K. P., Greene, E. and Irschick, D. J. (2008). Allometry of behavior. *Trends Ecol. Evol.* **23**, 394-401.

Dickinson, M. H. and Götz, K. G. (1996). The wake dynamics and flight forces of the fruit fly, *Drosophila melanogaster*. *J. Exp. Biol.* **199**, 2085-2104.

Ellington, C. P. (1999). The novel aerodynamics of insect flight: applications to micro-air vehicles. *J. Exp. Biol.* **202**, 3439-3448.

Felsenstein, J. (1985). Phylogenies and the comparative method. *Am. Nat.* **125**, 1-15.

Garland, T., Jr and Díaz-Uriarte, R. (1999). Polytomies and phylogenetically independent contrasts: an examination of the bounded degrees of freedom approach. *Syst. Biol.* **48**, 547-558.

Gatesy, S. M. and Baier, D. B. (2005). The origin of the avian flight stroke: a kinematic and kinetic perspective. *Paleobiology* **31**, 382-399.

Gelman, A. and Hill, J. (2007). *Data Analysis Using Regression and Multilevel/Hierarchical Models*. Cambridge: Cambridge University Press.

Giannini, N. P. and Simmons, N. B. (2005). Conflict and congruence in a combined DNA-morphology analysis of megachiropteran bat relationships (Mammalia: Chiroptera: Pteropodidae). *Cladistics* **21**, 411-437.

Greenewalt, C. H. (1975). The flight of birds: the significant dimensions, their departure from the requirements for dimensional similarity, and the effect of flight aerodynamics of that departure. *Trans. Am. Phil. Soc.* **65**, 1-67.

Hedenström, A., Johansson, L. C., Wolf, M., von Busse, R., Winter, Y. and Spedding, G. R. (2007). Bat flight generates complex aerodynamic tracks. *Science* **316**, 894-897.

Hedrick, T. L., Tobalske, B. W. and Biewener, A. A. (2002). Estimates of circulation and gait change based on a three-dimensional kinematic analysis of flight in cockatiels (*Nymphicus hollandicus*) and ringed turtle-doves (*Streptopelia risoria*). *J. Exp. Biol.* **205**, 1389-1409.

Hedrick, T. L., Tobalske, B. W. and Biewener, A. A. (2003). How cockatiels (*Nymphicus hollandicus*) modulate pectoralis power output across flight speeds. *J. Exp. Biol.* **206**, 1363-1378.

Heglund, N. C. and Taylor, C. R. (1988). Speed, stride frequency and energy cost per stride: how do they change with body size and gait? *J. Exp. Biol.* **138**, 301-318.

Hill, J. E. and Smith, S. A. (1981). *Craseonycteris thonglongyai*. *Mamm. Sp.* **160**, 1-4.

Hubel, T. Y., Hristov, N. I., Swartz, S. M. and Breuer, K. S. (2009). Time-resolved wake structure and kinematics of bat flight. *Exp. Fluids* **46**, 933-943.

Jones, D. P. and Kunz, T. H. (2000). *Pteropus hypomelanus*. *Mamm. Sp.* **639**, 1-6.

Jones, K. E., Purvis, A., MacLarnon, A., Bininda-Emonds, O. R. P. and Simmons, N. B. (2002). A phylogenetic supertree of the bats (Mammalia: Chiroptera). *Biol. Rev.* **77**, 223-259.

Kingston, T., Jones, G., Zubaid, A. and Kunz, T. H. (2000). Resource partitioning in rhinolophid bats revisited. *Oecologia* **124**, 332-342.

Kunz, T. H. and Jones, D. P. (2000). *Pteropus vampyrus*. Mamm. *Sp.* **642**, 1-6.

Kwiecinski, G. G. and Griffiths, T. A. (1999). *Pteropus hypomelanus*. *Mamm. Sp.* **611**, 1-9.

LaBarbera, M. (1989). Analyzing body size as a factor in ecology and evolution. *Annu. Rev. Ecol. Syst.* **20**, 97-117.

Lavin, S. R., Karasov, W. H., Ives, A. R., Middleton, K. M. and Garland, T., Jr (2008). Morphometrics of the avian small intestine compared with that of nonflying mammals: a phylogenetic approach. *Physiol. Biochem. Zool.* **81**, 526-550.

Liechti, F. and Bruderer, L. (2002). Wingbeat frequency of barn swallows and house martins: a comparison between free flight and wind tunnel experiments. *J. Exp. Biol.* **205**, 2461-2467.

Lindhe Norberg, U. M. and Winter, Y. (2006). Wing beat kinematics of a nectar-feeding bat, *Glossophaga soricina*, flying at different flight speeds and Strouhal numbers. *J. Exp. Biol.* **209**, 3887-3897.

Luft, S., Curio, E. and Tacud, B. (2003). The use of olfaction in the foraging behaviour of the golden-mantled flying fox, *Pteropus pumilus*, and the greater musky fruit bat, *Ptenochirus jagori* (Megachiroptera: Pteropodidae). *Naturwissenshaften* **90**, 84-87.

McGahan, J. (1973). Gliding flight of the Andean condor in nature. *J. Exp. Biol.* **58**, 225-237.

Miller, L. A. and Peskin, C. S. (2005). A computational fluid dynamics of 'clap and fling' in the smallest insects. *J. Exp. Biol.* **208**, 195-212.

Muijres, F. T., Johansson, L. C., Barfield, R., Wolf, M., Spedding, G. R. and Hedenström, A. (2008). Leading-edge vortex improves lift in slow-flying bats. *Science* **319**, 1250-1253.

Norberg, U. M. (1976). Kinematics, aerodynamics and energetics of horizontal flapping flight in the long-eared bat (*Plecotus auritus*). *J. Exp. Biol.* **65**, 179-212.

Norberg, U. M. (1981). Allometry of bat wings and legs and comparison with bird wings. *Philos. Trans. R. Soc. Lond. B Biol. Sci.* **292**, 359-368.

Norberg, U. M. (1990). *Vertebrate Flight*. Berlin: Springer-Verlag.

Norberg, U. M. and Rayner, J. M. V. (1987). Ecological morphology and flight in bats (Mammalia; Chiroptera): wing adaptations, flight performance, foraging strategy and echolocation. *Philos. Trans. R. Soc. Lond. B. Biol. Sci.* **316**, 335-427.

Nowak, R. M. (1994). *Walker's Bats of the World*. Baltimore: Johns Hopkins University Press.

Nudds, R. L. (2007). Wing-bone length allometry in birds. *J. Avian Biol.* **38**, 515-519.

O'Brien, J., Mariani, C., Olson, L., Russell, A. L., Say, L., Yoder, A. D. and Hayden, T. J. (2009). Multiple colonisations of the western Indian Ocean by *Pteropus* fruit bats (Megachiroptera: Pteropodidae): the furthest islands were colonised first. *Mol. Phylogenet. Evol.* **51**, 294-303.

Pagel, M. D. (1992). A method for the analysis of comparative data. *J. Theor. Biol.* **156**, 431-442.

Pennycuick, C. J. (1975). Mechanics of flight. In *Avian Biology*, Vol. 5 (ed. D. S. Farner and J. R. King), pp. 1-75. New York: Academic Press.

Purvis, A. and Garland, T., Jr (1993). Polytomies in comparative analyses of continuous characters. *Syst. Biol.* **42**, 569-575.

R Development Core Team (2009). *R: A Language and Environment for Statistical Computing*. Vienna, Austria: R Foundation for Statistical Computing.

Riskin, D. K., Willis, D. J., Iriarte-Díaz, J., Hedrick, T. L., Kostandov, M., Chen, J., Laidlaw, D. H., Breuer, K. S. and Swartz, S. M. (2008). Quantifying the complexity of bat wing kinematics. *J. Theor. Biol.* **254**, 604-615.

Sane, S. P. (2003). The aerodynamics of insect flight. *J. Exp. Biol.* **206**, 4191-4208.

Smith, R. J. (1984). Allometric scaling in comparative biology: problems of concept and method. *Am. J. Physiol.* **246**, R152-R160.

Storey, J.D. (2002). A direct approach to false discovery rates. *J. R. Stat. Soc. B* **64**, 479–498.

Surlykke, A., Miller, L. A., Møhl, B., Andersen, B. B., Christensen-Dalsgaard, J. and Jørgensen, M. B. (1993). Echolocation in two very small bats from Thailand: *Craseonycteris thonglongyai* and *Myotis siligorensis*. *Behav. Ecol. Sociobiol.* **33**, 1-12.

Taylor, G. K., Nudds, R. L. and Thomas, A. L. R. (2003). Flying and swimming animals cruise at a Strouhal number tuned for high power efficiency. *Nature* **425**, 707-711.

Teeling, E. C., Springer, M. S., Madsen, O., Bates, P., O'Brien, S. J. and Murphy, W. J. (2005). A molecular phylogeny for bats illuminates biogeography and the fossil record. *Science* **307**, 580-584.

Tobalske, B. W., Olson, N. E. and Dial, K. P. (1997). Flight style of the black-billed magpie: variation in wing kinematics, neuromuscular control and muscle composition. *J. Exp. Zool.* **279**, 313-329.

Tobalske, B. W., Warrick, D. R., Clark, C. J., Powers, D. R., Hedrick, T. L., Hyder, G. A. and Biewener, A. A. (2007). Three-dimensional kinematics of hummingbird flight. *J. Exp. Biol.* **210**, 2368-2382.

Warrick, D. R., Tobalske, B. W. and Powers, D. P. (2005). Aerodynamics of the hovering hummingbird. *Nature* **435**, 1094-1097.

Wilson, D. E. and Reeder, D. M. (1993). *Mammal Species of The World: a Taxonomic and Geographic Reference*. Washington: Smithsonian Institute Press.

filename	species	individual	mass(kg)	max_span_tw	min_span_tw	max_chord(m	max_area_tw	min_wing_loa	Aspect_Ratio	V_horiz(m·s^	V_vert(m·s^-	A_horiz(m·s^	A_vert(m·s^-	Wingbeat_Per	Downstroke_[	Downstroke_F	Wing_Stroke	Strouhal_Nur	Stroke_Plane	Wing_Camber	Angle_of_Atta	alpha1(deg.)	alpha2(deg.)	Coefficient_of_Lift
2006-07-11 c	Cynopterus br	cbry	0.0278	0.34902	0.11432	0.076823	0.022464	12.1404	5.4229	3.4544	0.1365	-0.94234	1.9423	0.111	0.052527	0.47321	72.9735	0.40706	-46.5977	0.065334	23.8668	10.3388	13.5281	1.0454
2006-07-11 c	Cynopterus br	cbry	0.0278	0.33083	0.16004	0.077512	0.022282	12.2396	4.912	4.3825	0.016927	0.72764	-1.5236	0.123	0.058524	0.47581	71.8431	0.34888	-63	0.040824	17.0277	1.0513	15.9764	0.63583
2006-07-11 c	Cynopterus br	cbry	0.0278	0.33566	0.16794	0.07785	0.022245	12.2598	5.0649	3.5491	0.029195	0.068293	0.47967	0.123	0.0615	0.5	71.4628	0.43062	-61.9077	0.0087776	17.4369	-1.9122	19.349	0.98374
2006-07-11 c	Cynopterus br	cbry	0.0278	0.3417	0.13137	0.077991	0.022556	12.0906	5.1764	6.4525	-0.35678	0.71905	-0.53095	0.126	0.064488	0.51181	72.0761	0.22117	-71.9827	0.017541	9.5314	-7.2916	16.823	0.38941
2006-07-11 c	Cynopterus br	cbry	0.0278	0.31945	0.097368	0.07819	0.020947	13.0194	4.8718	7.8366	-0.26103	-0.22098	-0.62797	0.143	0.062563	0.4375	74.6641	0.16809	-65.6285	-0.019236	9.2723	-3.2822	12.5545	0.27765
2006-07-06 c	Cynopterus br	cbor	0.031	0.35272	0.2127	0.076542	0.022953	13.2495	5.4205	3.5587	-0.008811	-0.53937	-0.27638	0.127	0.059531	0.46875	56.9268	0.32301	-48.0097	0.042501	19.4034	6.8784	12.525	0.9052
2006-07-06 c	Cynopterus br	cbor	0.031	0.34213	0.13251	0.077216	0.022613	13.4484	5.1763	4.8524	-0.061197	0.26515	-2.5705	0.132	0.060541	0.45865	87.812	0.31512	-63.0296	0.037179	15.1148	-0.8601	15.9749	0.4797
2006-07-06 c	Cynopterus br	cbor	0.031	0.34695	0.16826	0.07931	0.023344	13.0274	5.1565	4.672	-0.53999	1.2887	-1.6983	0.115	0.054526	0.47414	72.7768	0.3495	-64.5524	0.010972	15.1815	-7.0689	22.2504	0.55161
2006-07-06 c	Cynopterus br	cbor	0.031	0.34917	0.11532	0.078534	0.023157	13.1325	5.265	5.1731	-0.28954	0.98198	-3.1432	0.111	0.052527	0.47321	66.663	0.34406	-62.5655	0.016303	11.7482	-5.3378	17.086	0.36327
2006-07-06 c	Cynopterus br	cbor	0.031	0.34827	0.17426	0.07989	0.02338	13.0072	5.1879	6.4139	-0.19614	-0.095763	0.27373	0.118	0.056521	0.47899	70.9254	0.21767	-66.6588	0.0045338	8.0932	-7.2291	15.3223	0.43495
2006-07-17 c	Cynopterus br	cbdg	0.0345	0.37788	0.19841	0.082062	0.025451	13.2979	5.6106	3.3335	0.36909	-1.2057	-0.91557	0.122	0.057528	0.47154	65.7557	0.35706	-43.2314	0.063568	26.1978	16.6214	9.5764	0.9364
2006-07-17 c	Cynopterus br	cbdg	0.0345	0.37478	0.14915	0.083888	0.025798	13.1191	5.4445	4.3094	-0.0037466	2.1329	-7.2705	0.146	0.078463	0.53741	86.9726	0.37526	-58.1492	0.0013447	12.2377	-3.0492	15.2869	0.17934
2006-07-17 c	Cynopterus br	cbdg	0.0345	0.36336	0.056794	0.089867	0.02719	12.4473	4.8559	7.1151	-0.17235	0.54138	-5.7009	0.116	0.051556	0.44444	110.2782	0.33307	-68.0052	-0.070954	4.2483	-18.5107	22.759	0.1325
2006-07-17 c	Cynopterus br	cbdg	0.0345	0.37303	0.096972	0.083258	0.026354	12.8421	5.2801	6.2515	0.65448	-0.27463	-3.8037	0.134	0.056578	0.42222	81.0591	0.27904	-57.7341	0.0037023	6.9579	1.4474	5.5106	0.22429
2006-07-17 c	Cynopterus br	cbdg	0.0345	0.37611	0.073726	0.085106	0.026454	12.7939	5.3473	6.239	0.6787	-0.20455	0.21439	0.132	0.061534	0.46617	88.2917	0.27252	-53.5252	0.011465	13.6688	3.8038	9.865	0.36622
2006-07-13 c	Cynopterus br	cbma	0.035	0.35036	0.076812	0.078631	0.023982	14.3173	5.1186	3.7976	0.22945	-1.747	0.7735	0.117	0.060483	0.51695	84.0219	0.35261	-36.0604	0.079034	30.5875	19.4765	11.1111	0.69792
2006-07-13 c	Cynopterus br	cbma	0.035	0.36859	0.11901	0.077954	0.025207	13.6211	5.3896	3.2081	0.37689	0.35243	1.0631	0.103	0.046548	0.45192	84.8402	0.43293	-33.3166	0.088028	26.9459	13.6482	13.2977	0.88764
2006-07-13 c	Cynopterus br	cbma	0.035	0.35224	0.10069	0.078877	0.024095	14.2501	5.1494	4.7478	0.25893	0.15	0.16132	0.106	0.055477	0.52336	81.8696	0.36693	-50.6144	0.038589	20.6126	5.1432	15.4694	0.58349
2006-07-13 c	Cynopterus br	cbma	0.035	0.34788	0.097678	0.079166	0.023838	14.4035	5.0767	6.2133	0.48194	-0.073958	-0.61667	0.096	0.046515	0.48454	72.1708	0.34488	-68.6916	0.026632	16.5168	2.0839	14.4329	0.424
2006-07-13 c	Cynopterus br	cbma	0.035	0.35922	0.068064	0.079308	0.023804	14.4238	5.4209	7.4563	0.15665	0.5125	0.95417	0.096	0.044536	0.46392	89.6666	0.30518	-66.9604	0.013356	15.2707	0.71893	14.5517	0.38976
2006-07-18 c	Cynopterus br	cbyr	0.0395	0.40724	0.11671	0.083057	0.027996	13.8409	5.9238	5.5584	-0.50367	1.2068	-0.55782	0.147	0.064561	0.43919	79.6958	0.32812	-72.7599	0.11585	12.3197	-9.745	22.0647	0.5064
2006-07-18 c	Cynopterus br	cbyr	0.0395	0.41459	0.14249	0.084313	0.028719	13.4928	5.9852	7.518	-0.49735	1.1807	2.8606	0.109	0.055491	0.50909	71.4393	0.26121	-82.7498	0.08361	11.1289	-10.0317	21.1607	0.48734
2006-07-18 c	Cynopterus br	cbyr	0.0395	0.40212	0.14717	0.084026	0.027997	13.8405	5.7756	7.6832	-0.010642	-0.0089552	1.2291	0.134	0.061541	0.45926	87.6982	0.25234	-74.5898	0.032382	6.5712	-7.1833	13.7545	0.37773
2006-07-18 c	Cynopterus br	cbyr	0.0395	0.39201	0.28201	0.08383	0.027622	14.0284	5.5633	5.5078	0.1944	-1.844	2.3206	0.141	0.079437	0.56338	45.715	0.15958	-45.1942	0.08346	14.5616	8.8464	5.7152	0.74665
2006-07-18 c	Cynopterus br	cbyr	0.0395	0.36453	0.14036	0.083789	0.026821	14.4473	4.9542	7.313	0.40934	-0.65109	-0.013139	0.137	0.055594	0.4058	62.0114	0.21088	-61.9969	0.035964	9.126	3.8595	5.2665	0.38826
2007-07-16 r	Rousettus aec	rawb	0.112	0.57375	0.16447	0.10602	0.051626	21.2824	6.3765	4.1509	-0.20667	0.29556	1.4141	0.135	0.071471	0.52941	73.4361	0.47718	-55.9654	0.15958	25.662	1.6713	23.9907	1.1841
2007-07-16 r	Rousettus aec	rawb	0.112	0.53683	0.22634	0.10106	0.049297	22.2878	5.8459	3.4799	-0.17056	0.95391	0.275	0.128	0.064496	0.50388	61.048	0.5137	-45.8437	0.14634	18.827	-1.1681	19.9951	1.2934
2007-07-16 r	Rousettus aec	rawb	0.112	0.55709	0.24006	0.10346	0.050102	21.9298	6.1943	5.2112	-0.32138	-0.083333	0.88472	0.144	0.077462	0.53793	69.7548	0.34741	-70.1523	0.10707	20.3013	-2.945	23.2463	1.0427
2007-07-16 r	Rousettus aec	rawb	0.112	0.53301	0.20433	0.11314	0.053544	20.5198	5.3058	4.6644	-0.45075	1.0694	2.7685	0.124	0.065472	0.528	64.2995	0.52805	-71.2625	0.13223	22.8988	-4.873	27.7718	1.0462
2007-07-16 r	Rousettus aec	rawb	0.112	0.51726	0.20003	0.11275	0.048921	22.459	5.4693	4.2712	-0.48725	2.0812	-3.2329	0.149	0.067547	0.45333	60.2942	0.45204	-70.4973	0.11786	14.9002	-10.2722	25.1724	0.86584
2007-07-16 r	Rousettus aec	rayb	0.132	0.57409	0.22737	0.11434	0.063237	20.4773	5.2118	4.7875	-0.10874	1.1537	0.64027	0.149	0.0745	0.5	80.0962	0.47524	-65.3896	0.13805	20.3955	0.91999	19.4755	0.96329
2007-07-16 r	Rousettus aec	rayb	0.132	0.59117	0.13031	0.10984	0.062026	20.8769	5.6343	3.6845	-0.48004	2.9913	-0.142	0.15	0.074503	0.49669	72.4467	0.58546	-59.9175	0.16159	32.1034	0.61296	31.4904	0.99266
2007-07-16 r	Rousettus aec	rayb	0.132	0.58475	0.19024	0.1104	0.063072	20.5308	5.4213	4.2592	-1.1132	3.9147	-0.14825	0.143	0.072493	0.50694	80.238	0.56809	-76.7943	0.11181	29.7044	-10.8875	40.5919	0.89914
2007-07-16 r	Rousettus aec	rayb	0.132	0.62086	0.13465	0.11172	0.060877	21.271	6.332	3.9971	-0.70168	3.3497	-2.0206	0.155	0.076506	0.49359	100.8489	0.61419	-74.6903	0.12995	32.3657	-11.7497	44.1154	0.78358
2007-07-16 r	Rousettus aec	rayb	0.132	0.58847	0.19467	0.12013	0.059801	21.6539	5.7909	3.746	-0.43435	1.7093	-1.2464	0.151	0.0755	0.5	82.5682	0.57317	-60.54	0.16673	21.7508	-9.2832	31.034	0.99946
2007-07-16 r	Rousettus aec	ralg	0.159	0.54226	0.17855	0.1062	0.058431	26.6943	5.0323	4.3008	-0.01198	-0.34768	-0.79669	0.151	0.070533	0.46711	74.8946	0.45284	-58.6145	0.12348	27.6236	7.8071	19.8165	1.0011
2007-07-16 r	Rousettus aec	ralg	0.159	0.55792	0.28724	0.10684	0.058634	26.602	5.3088	4.8172	-0.22606	-0.016667	0.57569	0.144	0.07349	0.51034	66.0726	0.38159	-58.7242	0.13783	22.9438	3.5289	19.415	1.0802
2007-07-16 r	Rousettus aec	ralg	0.159	0.54221	0.22298	0.10663	0.060988	25.5753	4.8205	4.5912	-0.04031	-0.057042	0.017606	0.142	0.070503	0.4965	71.5094	0.44694	-62.6153	0.11463	26.2923	4.7779	21.5144	1.0174
2007-07-16 r	Rousettus aec	ralg	0.159	0.56673	0.30062	0.10726	0.05974	26.1094	5.3762	5.1768	-0.65253	0.61698	-1	0.159	0.084469	0.53125	75.4718	0.36213	-78.1529	0.10953	24.2203	-3.1372	27.3575	0.96295
2007-07-16 r	Rousettus aec	ralg	0.159	0.54313	0.37509	0.10835	0.058849	26.505	5.0127	4.997	-0.41045	0.39128	-2.1477	0.149	0.076487	0.51333	49.5424	0.31479	-67.2363	0.096003	20.888	5.1869	15.701	0.92097
2007-07-25 r	Pteropus pum	pp223	0.178	0.73111	0.24201	0.13263	0.098495	17.7285	5.4268	3.7149	-0.014803	-1.1989	0.49438	0.178	0.081542	0.4581	75.8625	0.52482	-45.245	0.11782	36.4052	13.3302	23.075	0.7716
2007-07-25 r	Pteropus pum	pp223	0.178	0.71181	0.29519	0.13544	0.094948	18.3909	5.3363	4.0711	0.30568	-1.3102	0.98466	0.176	0.08452	0.48023	70.4635	0.48139	-46.8926	0.12327	33.3108	19.1704	14.1403	0.88459
2007-07-25 r	Pteropus pum	pp223	0.178	0.73962	0.39702	0.13663	0.098072	17.805	5.578	4.7276	0.16435	-0.83533	-0.22036	0.167	0.090458	0.54167	62.2366	0.39184	-46.7165	0.12791	28.5743	10.0678	18.5065	0.7301
2007-07-25 r	Pteropus pum	pp223	0.178	0.74122	0.26588	0.13902	0.097557	17.8991	5.6317	4.3783	-0.05622	0.52775	-0.12618	0.191	0.0955	0.5	82.0671	0.50287	-54.2692	0.12263	24.4266	1.143	23.2836	0.64275
2007-07-25 r	Pteropus pum	pp223	0.178	0.74325	0.2346	0.15946	0.096424	18.1095	5.729	4.0961	0.049253	-0.14301	1.1258	0.186	0.092503	0.49733	87.3691	0.53568	-53.3966	0.12013	30.8853	10.234	20.6512	0.85638
2007-07-25 r	Pteropus pum	pp311	0.178	0.6433	0.29204	0.13928	0.081074	21.5381	5.1045	3.7099	0.46712	-0.98366	-1.5366	0.153	0.068552	0.44805	41.4106	0.59567	-52.1644	0.13966	27.0966	24.527	2.5696	1.2272
2007-07-25 t	Pteropus pum	pp311	0.178	0.70749	0.17719	0.14223	0.085001	20.543	5.8886	5.699	-0.30993	2.4818	-0.59716	0.176	0.096452	0.54802	88.4633	0.43044	-72.2951	0.11507	24.6116	-5.4479	30.0596	0.60246
2007-07-25 r	Pteropus pum	pp311	0.178	0.70741	0.22727	0.1411	0.084182	20.7429	5.9445	5.4256	-0.027056	2.3307	-1.0927	0.179	0.094472	0.52778	97.7091	0.51776	-72.2679	0.11028	7.6296	-1.1358	8.7654	0.94997
2007-07-25 r	Pteropus pum	pp311	0.178	0.71263	0.20311	0.14756	0.085253	20.4823	5.9569	5.4313	-0.01411	1.7864	-0.88325	0.191	0.10147	0.53125	99.8262	0.47463	-73.4376	0.086276	15.666	-9.9798	25.6459	0.77191
2007-07-25 t	Pteropus pum	pp311	0.178	0.70308	0.20327	0.13781	0.081845	21.3353	6.0397	4.7572	-0.10895	2.2051	1.6983	0.175	0.09446	0.53977	90.8898	0.56578	-69.5164	0.16527	20.7299	0.23302	20.4969	1.3648
2007-07-25 r	Pteropus pum	ppmob	0.18	0.67491	0.3535	0.13577	0.088539	19.9439	5.1447	4.7917	0.096038	1.3615	-3.525	0.208	0.10649	0.51196	74.2378	0.3836	-63.7038	0.051953	30.9503	17.7059	13.2444	0.6627
2007-07-25 r	Pteropus pum	ppmob	0.18	0.75426	0.29977	0.13849	0.088374	19.981	6.4375	4.5037	-0.095616	1.133	0.74757	0.185	0.097473	0.52688	80.6639	0.46688	-57.5993	0.076591	30.0715	6.5651	23.5064	0.96366
2007-07-25 t	Pteropus pum	ppmob	0.18	0.67178	0.39591	0.13702	0.087652	20.1456	5.1487	5.187	-0.037113	0.27965	-3.0814	0.231	0.1384	0.59914	63.7433	0.3065	-63.8142	-0.032137	21.0746	7.1431	13.9314	0.66945
2007-07-25 r	Pteropus pum	ppmob	0.18	0.72612	0.22628	0.14567	0.08779	20.1139	6.0058	5.6605	0.22871	-1.3669	-1.7402	0.254	0.14642	0.57647	81.7437	0.23189	-50.0198	0.043486	23.6012	9.0943	14.5069	0.71884
2007-07-26 r	Pteropus pum	ppmob	0.18	0.73684	0.3151	0.14017	0.092028	19.1877	5.8997	6.0036	0.26677	-0.33962	0.22731	0.26	0.14943	0.57471	77.5933	0.25374	-69.0549	0.030524	18.2279	8.0753	10.1526	0.83829
2007-07-25 t	Pteropus pum	pp224	0.204	0.78801	0.24928	0.14344	0.10046	19.9215	6.1814	4.3927	-0.0030798	1.8596	1.7713	0.188	0.095492	0.50794	85.7915	0.56542	-63.9307	0.14971	19.6945	-2.2873	21.9818	1.1667
2007-07-25 r	Pteropus pum	pp224	0.204	0.77749	0.26535	0.15024	0.10446	19.1576	5.7866	4.3099	-0.051373	-0.45141	-4.3548	0.177	0.084522	0.47753	96.4579	0.67202	-68.5683	0.13906	22.5876	-5.9065	28.4942	0.42149
2007-07-25 r	Pteropus pum	pp224	0.204	0.76586	0.2937	0.14808	0.10335	19.364	5.6754	5.3067	0.029634	0.73005	-0.20845	0.213	0.12043	0.56542	100.9202	0.47197	-66.6201	0.061326	18.2708	5.2832	12.9876	0.70494
2007-07-25 r	Pteropus pum	pp224	0.204	0.77643	0.36789	0.14441	0.096419	20.7557	6.5224	4.0637	0.26015	-2.7483	-0.57191	0.178	0.10342	0.58101	64.9584	0.27342	-14.2416	0.068837	26.7751	21.8894	4.8857	0.99252
2007-07-25 r	Pteropus pum	pp224	0.204	0.7741	0.24351	0.14426	0.10724	18.6617	5.5879	4.7178	-0.17021	0.12632	2.1853	0.19	0.091518	0.48168	92.2777	0.54964	-66.1876	0.11987	22.1971	-4.8105	27.0076	0.83616
2007-07-26 t	Pteropus pum	ppmby	0.212	0.76072	0.54011	0.14395	0.098665	21.0785	5.8653	4.5052	-0.26039	-1.66	-0.54	0.19	0.11141	0.58639	44.9638	0.23938	-45.5104	0.12205	26.6333	14.1135	12.5198	1.0631
2007-07-26 r	Pteropus pum	ppmby	0.212	0.75172	0.2044	0.14385	0.10093	20.6061	5.599	3.2103	0.34319	3.1905	-1.6101	0.168	0.074556	0.44379	82.5513	0.86142	-60.7977	0.089796	23.8008	-6.8499	30.6507	0.83034
2007-07-26 r	Pteropus pum	ppmby	0.212	0.73514	0.51072	0.14325	0.098058	21.2092	5.5114	4.8099	-0.10431	-0.56211	-0.66842	0.19	0.10942	0.57592	43.117	0.25908	-50.0618	0.067622	19.2947	9.3777	9.917	0.96329
2007-07-26 t	Pteropus pum	ppmby	0.212	0.77173	0.45718	0.14405	0.097541	21.3215	6.1058	4.9822	-0.00043889	-1.3294	2.0406	0.18	0.099448	0.55249	65.2223	0.32537	-48.7348	0.085483	22.9693	4.204	18.7653	0.92619
2007-07-26 r	Pteropus pum	ppmby	0.212	0.7623	0.33892	0.15619	0.097657	21.2961	5.9505	5.0128	0.11843	1.1557	1.1809	0.183	0.089511	0.48913	78.7808	0.45791	-63.0384	0.07486	18.391	-8.4705	26.8615	0.96515
2007-07-14 e	Eidolon helvur	eh301	0.254	0.81943	0.15776	0.12983	0.10373	24.0223	6.4735	3.4991	-0.4075	0.86269	-0.37313	0.201	0.09851	0.4901	90.8317	0.57934	-46.8166	0.078274	41.1102	14.8067	26.3035	0.89303
2007-07-14 e	Eidolon helvur	eh301	0.254	0.81061	0.25728	0.12959	0.099199	25.1186	6.624	4.4178	0.36096	-1.1152	0.64242	0.198	0.10945	0.55276	82.2595	0.40275	-39.654	0.10937	29.2573	13.9699	15.2875	0.93193
2007-07-14 e	Eidolon helvur	eh301	0.254	0.79212	0.14463	0.13243	0.098492	25.2989	6.3706	2.3502	0.56937	-0.66243	-1.9597	0.181	0.092489	0.51099	93.3916	0.67251	-32.304	0.086328	41.2041	26.6154	14.5887	1.1761
2007-07-14 e	Eidolon helvur	eh301	0.254	0.8063	0.22262	0.13351	0.094433	26.3862	6.8845	4.1282	0.15467	-0.38698	-0.75677	0.192	0.10048	0.52332	83.9341	0.44301	-37.2763	0.09308	30.641	8.7655	21.8755	0.78468
2007-07-14 e	Eidolon helvur	eh301	0.254	0.81582	0.18811	0.1375	0.099802	24.9669	6.6688	4.5667	-0.21167	-0.32279	-0.27302	0.215	0.11148	0.51852	79.1312	0.364	-43.9732	0.037898	32.3544	13.1756	19.1788	0.95617
2007-07-15 e	Eidolon helvur	eh348	0.266	0.79422	0.38435	0.13656	0.10437	25.0013	6.0435	6.0913	0.014355	-0.080087	0.77403	0.231	0.11749	0.50862	77.603	0.31172	-61.9342	0.10313	27.063	11.7152	15.3478	0.88717
2007-07-15 e	Eidolon helvur	eh348	0.266	0.81791	0.38224	0.14102	0.10313	25.3019	6.4866	5.4251	0.096542	-1.9147	0.49244	0.238	0.13344	0.56067	84.2285	0.28883	-44.443	0.1239	29.8223	14.8182	15.0041	0.89821
2007-07-15 e	Eidolon helvur	eh348	0.266	0.80407	0.25045	0.13742	0.10343	25.2303	6.2511	4.4316	0.13984	0.094472	0.37035	0.199	0.098505	0.495	82.8966	0.48353	-48.85	0.14693	24.7925	9.4851	15.3074	1.0145
2007-07-15 e	Eidolon helvur	eh348	0.266	0.76024	0.16605	0.14739	0.10568	24.6918	5.4689	3.4723	0.24822	0.74895	-0.32368	0.19	0.087539	0.46073	64.5334	0.60119	-47.674	0.13241	29.2174	16.799	12.4184	1.4455
2007-07-15 e	Eidolon helvur	eh348	0.266	0.80397	0.26377	0.13645	0.10569	24.6889	6.1154	5.2882	0.45054	-0.59821	0.46607	0.224	0.10951	0.48889	76.2655	0.32717	-53.456	0.10598	21.4786	12.5788	8.8998	0.97082
2007-07-14 e	Eidolon helvur	eh356	0.278	0.75558	0.20572	0.13828	0.10563	25.8185	5.4048	4.3756	0.48245	0.65176	-0.91765	0.17	0.085497	0.50292	85.817	0.59022	-50.3835	0.19716	35.4303	16.7408	18.6895	0.81472
2007-07-14 e	Eidolon helvur	eh356	0.278	0.77538	0.30247	0.13961	0.10494	25.9883	5.7291	4.9418	0.42373	-0.60276	-0.63702	0.181	0.088511	0.48901	75.3224	0.4233	-50.8456	0.21535	32.2691	18.188	14.0811	0.84394
2007-07-14 e	Eidolon helvur	eh356	0.278	0.7691	0.22094	0.1435	0.1074	25.3931	5.5077	5.1077	0.34826	-0.76573	-0.6427	0.178	0.089497	0.50279	87.7024	0.47676	-53.3226	0.20024	28.7585	7.4304	21.3281	0.79105
2007-07-14 e	Eidolon helvur	eh356	0.278	0.75449	0.26286	0.14026	0.1021	26.7105	5.5754	4.6035	0.65506	0.058757	-0.76723	0.177	0.087506	0.49438	83.0999	0.44884	-43.3234	0.17925	29.3956	16.2025	13.1931	0.83365
2007-07-14 e	Eidolon helvur	eh356	0.278	0.78422	0.22342	0.15192	0.10509	25.9499	5.8519	5.057	0.49023	-3.0351	0.99681	0.188	0.091513	0.48677	92.7813	0.47564	-56.3626	0.23004	32.0111	13.3633	18.6478	0.91931
2007-07-15 e	Eidolon helvur	ehrw	0.326	0.90615	0.24237	0.14512	0.12537	25.5087	6.5495	3.495	0.63792	-1.1671	0.093237	0.207	0.11047	0.53365	91.3475	0.54347	-39.4478	0.21057	30.0618	21.5379	8.5239	1.1545
2007-07-15 e	Eidolon helvur	ehrw	0.326	0.88233	0.25469	0.15041	0.12568	25.4454	6.1942	2.8145	-0.051083	-0.29482	-0.05285	0.193	0.095505	0.49485	78.4345	0.70003	-36.412	0.16518	36.8902	20.4538	16.4364	1.1274
2007-07-15 e	Eidolon helvur	ehrw	0.326	0.88563	0.26406	0.14976	0.12358	25.8784	6.3469	3.6954	0.24918	-1.0492	0.19949	0.195	0.10247	0.52551	78.9949	0.57288	-42.7883	0.16987	33.6753	20.1282	13.5471	1.1364
2007-07-15 e	Eidolon helvur	ehrw	0.326	0.9028	0.28377	0.16218	0.12512	25.5609	6.5144	3.2949	0.40638	0.11058	-0.84567	0.208	0.10649	0.51196	80.8971	0.56032	-40.7902	0.15974	27.2243	15.1852	12.0392	1.3183
2007-07-15 e	Eidolon helvur	ehrw	0.326	0.87831	0.33882	0.15182	0.12808	24.9701	6.0233	3.8694	0.31984	-0.79348	0.22337	0.184	0.094486	0.51351	63.164	0.54791	-46.4148	0.14389	25.8807	18.3011	7.5795	1.4314
2007-07-17 e	Eidolon helvur	eh391	0.332	0.82855	0.25312	0.1432	0.11325	28.7588	6.0618	4.5456	0.31673	1.2348	-0.49314	0.204	0.11145	0.54634	78.2949	0.57118	-51.637	0.25066	35.3193	18.287	17.0323	0.94896
2007-07-17 e	Eidolon helvur	eh391	0.332	0.81347	0.37084	0.13435	0.10716	30.3926	6.1751	4.7842	0.73621	-1.7071	-1.4434	0.196	0.10148	0.51777	73.8998	0.39682	-44.2507	0.15592	34.4628	27.4992	6.9636	0.94296
2007-07-17 e	Eidolon helvur	eh391	0.332	0.83435	0.27085	0.13575	0.1092	29.8246	6.3747	3.8224	0.48181	-2.1954	-2.6933	0.195	0.1164	0.59694	69.252	0.31594	-21.9114	0.22987	36.0952	31.635	4.4602	0.84965
2007-07-17 e	Eidolon helvur	eh391	0.332	0.8415	0.22823	0.16013	0.10997	29.616	6.4391	5.0618	0.47397	0.23416	-0.42772	0.202	0.097517	0.48276	102.4684	0.48859	-52.1843	0.21641	32.9963	15.4314	17.5649	0.83945
2007-07-17 e	Eidolon helvur	eh391	0.332	0.82838	0.19185	0.13436	0.10801	30.1552	6.3535	2.8247	-0.061006	0.29818	0.30485	0.165	0.0825	0.5	82.558	0.74773	-30.8632	0.25108	33.908	19.2305	14.6775	1.3
2007-07-21 r	Pteropus hypc	ph219	0.454	1.0554	0.40082	0.19286	0.18391	24.2169	6.0565	4.7231	-0.15029	1.2023	-0.25509	0.216	0.11447	0.52995	78.4776	0.62087	-59.7821	0.1533	30.3581	0.65415	29.7039	0.76245
2007-07-21 r	Pteropus hypc	ph219	0.454	1.024	0.34452	0.21786	0.19945	22.33	5.2569	4.8936	0.33011	-0.16039	-0.65647	0.255	0.14344	0.5625	73.8579	0.53898	-60.8233	0.15522	23.0721	4.6208	18.4513	0.87867
2007-07-21 r	Pteropus hypc	ph219	0.454	1.0128	0.27498	0.22496	0.20044	22.2193	5.1174	5.6352	0.68127	-1.0719	0.89663	0.267	0.1604	0.60075	97.9301	0.4723	-63.0186	0.11583	24.8091	13.6719	11.1372	0.85885
2007-07-21 r	Pteropus hypc	ph219	0.454	1.0599	0.28702	0.19597	0.1901	23.4279	5.9099	5.8795	0.35012	0.66069	-0.11724	0.29	0.15945	0.54983	91.0596	0.41037	-70.7767	0.14732	30.7066	10.6672	20.0394	0.77674
2007-07-21 t	Pteropus hypc	ph219	0.454	1.0625	0.24548	0.19905	0.21595	20.6238	5.2279	6.0242	0.7653	2.9369	-2.4183	0.301	0.16645	0.55298	105.3287	0.43264	-68.6036	0.044578	29.4718	11.0505	18.4212	0.45885
2007-07-24 r	Pteropus hypc	ph251	0.464	1.0494	0.42361	0.19512	0.18241	24.9533	6.0371	5.488	0.17769	1.126	-0.40681	0.235	0.12746	0.54237	79.5496	0.54838	-66.9767	0.13147	22.7115	3.4495	19.262	0.72756
2007-07-24 r	Pteropus hypc	ph251	0.464	1.0622	0.3482	0.21358	0.19473	23.375	5.7935	5.4465	0.59671	0.17633	-0.59329	0.283	0.16243	0.57394	90.6107	0.44024	-59.1585	0.092554	22.8773	10.3712	12.5061	0.81405
2007-07-24 t	Pteropus hypc	ph251	0.464	1.0692	0.31612	0.21144	0.19484	23.3619	5.8677	5.3207	0.073131	2.012	-1.1067	0.283	0.15645	0.55282	99.4871	0.46421	-65.9086	0.11274	19.4691	-1.7307	21.1997	0.75295
2007-07-24 r	Pteropus hypc	ph251	0.464	1.0713	0.37083	0.2041	0.18316	24.8517	6.2662	5.4234	0.11652	1.3192	-0.64962	0.26	0.14544	0.55939	87.7504	0.48213	-62.3541	0.094259	21.4072	0.79672	20.6105	0.80096
2007-07-24 r	Pteropus hypc	ph251	0.464	1.0782	0.34714	0.20017	0.1891	24.0713	6.1477	5.5698	0.14962	0.38192	-0.38672	0.271	0.14646	0.54044	82.5862	0.46676	-64.6278	0.12365	21.9802	1.0079	20.9722	0.74294
2007-07-21 t	Pteropus hypc	ph202	0.468	1.0061	0.5181	0.18596	0.1674	27.4262	6.0473	5.0604	0.25405	-2.0687	-0.36796	0.284	0.1714	0.60351	78.3084	0.32493	-45.4029	0.10372	24.0121	8.3505	15.6617	0.90185
2007-07-21 r	Pteropus hypc	ph202	0.468	1.0152	0.24557	0.18325	0.16656	27.5636	6.1871	3.903	0.32895	0.11789	0.33303	0.218	0.10651	0.48858	93.5708	0.66165	-53.5634	0.14316	34.2692	14.533	19.7362	1.33
2007-07-21 r	Pteropus hypc	ph202	0.468	1.0106	0.24811	0.18883	0.16628	27.6101	6.1415	5.9413	0.73225	2.2154	-1.6921	0.267	0.14446	0.54104	95.7462	0.39554	-66.7921	0.12424	28.9917	11.0226	17.9691	0.73852
2007-07-21 t	Pteropus hypc	ph202	0.468	1.0248	0.31896	0.19552	0.17486	26.255	6.0055	6.0252	0.66452	1.2021	-0.25801	0.281	0.15744	0.56028	91.0051	0.3587	-64.6502	0.1109	23.4139	8.5167	14.8972	0.97928
2007-07-21 r	Pteropus hypc	ph202	0.468	1.0136	0.35634	0.17994	0.15965	28.7569	6.435	5.6465	0.4239	-0.39084	-0.052381	0.273	0.15344	0.56204	88.9553	0.36773	-60.7448	0.1021	25.9986	9.8917	16.1069	1.0009
2007-07-20 r	Pteropus hypc	ph256	0.49	1.0446	0.28754	0.23498	0.18647	25.7786	5.8523	6.3779	0.21832	1.4371	-1.2006	0.313	0.17245	0.55096	95.1517	0.35517	-74.2805	0.098583	28.8402	9.1951	19.6452	0.81677
2007-07-20 r	Pteropus hypc	ph256	0.49	1.0442	0.28929	0.19451	0.18671	25.7457	5.8401	6.6325	0.34498	0.20164	0.31776	0.304	0.16845	0.5541	100.5325	0.3592	-69.373	0.10481	24.9641	5.2249	19.7392	0.79449
2007-07-20 r	Pteropus hypc	ph256	0.49	1.0624	0.31793	0.19873	0.19905	24.1493	5.6705	6.1205	0.16931	1.0632	-0.53453	0.307	0.17443	0.56818	98.1718	0.38205	-68.6327	0.091007	21.3615	1.5312	19.8303	0.87756
2007-07-23 t	Pteropus hypc	ph256	0.49	1.0225	0.32099	0.19217	0.19057	25.2238	5.4864	5.5558	0.21322	-0.02963	0.77071	0.297	0.16544	0.55705	96.7766	0.42982	-69.0088	0.13932	27.0357	5.5788	21.457	1.1288
2007-07-23 r	Pteropus hypc	ph256	0.49	1.0328	0.33182	0.20894	0.20943	22.9527	5.093	5.9167	0.12865	1.7043	-1.392	0.276	0.13451	0.48736	92.2755	0.43314	-72.3058	0.094476	20.1155	-0.50127	20.6168	0.69107
2007-07-21 r	Pteropus hypc	ph255	0.526	1.0184	0.26625	0.27705	0.21309	24.2159	4.8676	5.5195	0.21676	-0.0020528	-2.3009	0.341	0.17549	0.51462	112.6339	0.40928	-75.204	0.091448	22.6937	7.4351	15.2586	0.76686
2007-07-21 t	Pteropus hypc	ph255	0.526	1.0886	0.34888	0.20897	0.1995	25.8654	5.9406	5.7266	0.53576	-0.43681	0.4273	0.326	0.18045	0.55352	86.4305	0.35971	-64.7912	0.1166	23.9132	8.7923	15.1209	0.89966
2007-07-21 r	Pteropus hypc	ph255	0.526	1.1002	0.3288	0.20797	0.20015	25.7813	6.0475	6.0218	0.038787	-0.49279	1.6483	0.319	0.18841	0.59062	83.5917	0.35212	-68.4227	0.10402	27.6733	11.836	15.8373	1.0695
2007-07-21 r	Pteropus hypc	ph255	0.526	1.0432	0.2925	0.20708	0.19794	26.0693	5.4975	6.2404	0.26531	-1.8206	-1.3854	0.316	0.1894	0.59937	104.615	0.41237	-74.14	0.02089	21.32	5.831	15.4889	0.70515
2007-07-21 t	Pteropus hypc	ph255	0.526	1.075	0.3284	0.21041	0.19739	26.1411	5.8542	5.839	-0.062981	0.9257	-0.75851	0.323	0.1954	0.60494	91.1528	0.39601	-71.4016	0.09387	28.6381	5.3967	23.2415	0.8286
2007-07-19 r	Pteropus vam	pv375	1.02	1.4013	0.46035	0.27712	0.34402	29.086	5.708	3.7421	0.075937	0.29193	-0.29404	0.285	0.15047	0.52797	77.2627	0.53963	-33.2584	0.083571	34.9239	16.5446	18.3794	1.2283
2007-07-19 r	Pteropus vam	pv375	1.02	1.4169	0.63347	0.25245	0.33215	30.1254	6.0446	4.2271	0.086842	-1.0974	-0.5652	0.273	0.14347	0.52555	62.4484	0.3695	-27.7879	0.10127	28.8596	19.0902	9.7694	0.9779
2007-07-19 t	Pteropus vam	pv375	1.02	1.4198	0.69844	0.24998	0.32746	30.5569	6.1558	4.9864	0.24974	-1.3327	0.18788	0.297	0.15747	0.5302	62.1534	0.275	-34.6493	0.089004	27.7147	14.7694	12.9453	1.0116
2007-07-19 r	Pteropus vam	pv375	1.02	1.4308	0.69607	0.25425	0.33677	29.7126	6.0794	5.2516	0.33563	-1.5643	0.59406	0.286	0.15247	0.5331	59.6748	0.3128	-36.766	0.091779	24.8336	12.1797	12.6539	0.99981
2007-07-19 r	Pteropus vam	pv375	1.02	1.3875	0.67051	0.25113	0.3327	30.0758	5.7868	5.6289	0.32294	-1.6758	0.24074	0.297	0.16345	0.55034	58.377	0.30075	-48.2739	0.049393	24.4384	15.9603	8.4781	0.99263
2007-07-19 t	Pteropus vam	pv625	1.052	1.423	0.53516	0.25826	0.36319	28.415	5.5753	5.4604	0.20985	-0.44321	0.38036	0.28	0.14947	0.53381	70.2158	0.48364	-64.238	0.086676	36.0292	10.6422	25.387	0.91589
2007-07-19 r	Pteropus vam	pv625	1.052	1.4429	0.49217	0.33849	0.40464	25.5046	5.145	6.1151	0.4256	2.8377	-1.5219	0.297	0.16744	0.56376	87.1725	0.49879	-69.6746	0.10694	31.9603	8.6309	23.3294	0.85311
2007-07-20 r	Pteropus vam	pv625	1.052	1.4474	0.45656	0.25845	0.35473	29.093	5.9062	6.2656	0.75139	-1.2361	1.2941	0.269	0.14745	0.54815	72.6373	0.3736	-44.1515	0.085084	34.7374	13.8249	20.9126	1.0328
2007-07-20 r	Pteropus vam	pv625	1.052	1.4287	0.52918	0.25477	0.34669	29.7678	5.888	5.9489	0.54717	-0.29191	0.81324	0.272	0.14845	0.54579	66.6156	0.38579	-55.6348	0.067525	36.9482	18.4347	18.5135	1.0946
2007-07-20 r	Pteropus vam	pv625	1.052	1.4564	0.52353	0.26406	0.35642	28.9545	5.9509	6.0551	0.69788	-0.70854	0.16797	0.281	0.15943	0.56738	64.3741	0.38119	-50.9805	0.087777	29.7411	12.3882	17.3529	0.96744
2007-07-23 t	Pteropus vam	pv608	1.09	1.5209	0.52039	0.29568	0.4204	25.4348	5.5025	5.1003	0.30466	-0.31705	3.6765	0.264	0.16139	0.61132	79.305	0.58385	-56.2708	0.13625	30.1169	10.3737	19.7432	1.2574
2007-07-23 r	Pteropus vam	pv608	1.09	1.5351	0.56421	0.27157	0.42222	25.3254	5.5813	4.8321	0.20775	1.712	2.1314	0.283	0.16641	0.58803	86.4947	0.60146	-53.2987	0.12314	30.5872	8.4358	22.1514	1.1611
2007-07-23 r	Pteropus vam	pv608	1.09	1.4938	0.5176	0.30492	0.4182	25.5687	5.336	4.3881	-0.18412	2.5236	2.0321	0.28	0.1674	0.59786	74.0516	0.70304	-55.9336	0.093437	39.0083	12.8607	26.1476	1.149
2007-07-23 t	Pteropus vam	pv608	1.09	1.4493	0.61803	0.30034	0.41099	26.0174	5.1108	5.0463	-0.094297	2.2802	2.9158	0.273	0.16241	0.59489	70.8923	0.58969	-54.7144	0.1672	36.9402	7.0246	29.9155	1.1739
2007-07-23 r	Pteropus vam	pv608	1.09	1.5146	0.46304	0.32277	0.40938	26.1199	5.604	4.5573	0.089706	1.8762	1.41	0.269	0.1604	0.5963	73.3223	0.63291	-53.544	0.1044	38.2609	13.1956	25.0654	1.0577
2007-07-24 r	Pteropus vam	pv365	1.152	1.4232	0.49836	0.27131	0.3518	32.1239	5.7579	5.5907	0.84105	1.4382	0.13166	0.259	0.14444	0.55769	76.2949	0.46379	-53.7114	0.034093	41.0553	18.5572	22.4981	1.127
2007-07-24 t	Pteropus vam	pv365	1.152	1.4468	0.50554	0.27546	0.35269	32.0425	5.9351	5.2717	0.025016	4.3398	-0.74488	0.254	0.13746	0.54118	71.2602	0.52427	-55.8645	0.07266	40.7256	14.8683	25.8573	1.321
2007-07-24 r	Pteropus vam	pv365	1.152	1.4637	0.49781	0.26433	0.35065	32.2291	6.1098	5.3872	0.18789	-0.36909	2.4553	0.275	0.16938	0.61594	77.8895	0.519	-57.1449	0.093679	38.7898	12.5825	26.2073	1.6463
2007-07-24 r	Pteropus vam	pv365	1.152	1.4104	0.49279	0.29275	0.34787	32.4862	5.7181	6.0105	-0.60137	3.3207	0.32714	0.28	0.16242	0.58007	82.8583	0.52205	-83.4742	0.091544	38.0629	11.575	26.4879	1.1538
2007-07-24 t	Pteropus vam	pv365	1.152	1.4335	0.42724	0.26775	0.35439	31.8893	5.7988	5.0181	0.20152	-0.5803	1.3004	0.264	0.14844	0.56226	78.0984	0.55596	-55.338	0.12255	43.7288	18.6606	25.0682	1.0525

Table S2A. Changes in wing kinematics with increases in V_{horiz}, with the influence of A_{horiz} and A_{vert} held constant

Species	*Cynopterus brachyotis* (d.f.=17)	*Rousettus aegyptiacus* (d.f.=9)	*Pteropus pumilus* (d.f.=17)	*Eidolon helvum* (d.f.=17)	*Pteropus hypomelanus* (d.f.=17)	*Pteropus vampyrus* (d.f.=17)
Maximum wingspan (b_{max})	Decrease					
	t=–2.51	t=0.07	t=1.35	t=1.30	t=1.06	t=–0.20
	P<0.034	P=0.95	P=0.20	P=0.21	P=0.30	P=0.85
Minimum wingspan (b_{min})	Decrease			Increase		Increase
	t=–2.62	t=1.96	t=0.96	t=3.93	t=–0.49	t=2.69
	P=0.0178	P=0.08	P=0.35	P=0.0011	P=0.63	P=0.019
Wingbeat period (T)			Increase	Increase	Increase	
	t=–0.48	t=2.00	t=4.09	t=4.80	t=3.43	t=1.28
	P=0.64	P=0.08	P<0.001	P<0.001	P<0.01	P=0.22
Downstroke period (T_{down})			Increase	Increase	Increase	
	t=–1.37	t=2.36	t=5.07	t=3.71	t=4.00	t=1.35
	P=0.19	P=0.04	P<0.0001	P<0.01	P<0.001	P=0.20
Downstroke ratio (τ)			Increase		Increase	
	t=–1.42	t=1.60	t=3.57	t=1.28	t=3.10	t=1.12
	P=0.18	P=0.14	P<0.01	P=0.22	P<0.01	P=0.28
Wing stroke amplitude (ϕ)						
	t=1.40	t=–0.02	t=1.95	t=–0.11	t=0.87	t=–0.81
	P=0.18	P=0.98	P=0.07	P=0.91	P=0.40	P=0.43
Stroke plane angle (β)	Decrease	Decrease	Decrease	Decrease	Decrease	
	t=–5.61	t=–6.36	t=–2.38	t=–4.08	t=–2.93	t=–1.84
	P<0.0001	P<0.001	P<0.034	P<0.001	P<0.01	P=0.09
Angle of attack (α)	Decrease		Decrease			Decrease
	t=–9.36	t=–1.04	t=–3.62	t=–1.81	t=–1.22	t=–4.08
	P<0.0001	P=0.32	P<0.01	P=0.09	P=0.24	P<0.01
α_1	Decrease		Decrease			
	t=–4.64	t=–1.33	t=–2.55	t=–2.16	t=1.03	t=–1.49
	P<0.001	P=0.22	P<0.034	P=0.05	P=0.32	P=0.16
α_2					Decrease	Decrease
	t=–0.43	t=0.24	t=0.20	t=0.24	t=–2.43	t=–2.68
	P=0.67	P=0.81	P=0.85	P=0.81	P<0.034	P<0.034
Wing camber	Decrease	Decrease		Decrease	Decrease	
	t=–5.56	t=–3.86	t=–1.88	t=–2.42	t=–2.63	t=–0.65
	P<0.0001	P<0.01	P=0.08	P<0.034	P<0.034	P=0.53
Strouhal number (St)	Decrease	Decrease	Decrease	Decrease	Decrease	Decrease
	t=–5.97	t=–4.37	t=–4.82	t=–8.59	t=–5.84	t=–4.97
	P<0.0001	P<0.01	P<0.001	P<0.0001	P<0.0001	P<0.001
Lift coefficient (C_L)	Decrease	Decrease	Decrease	Decrease	Decrease	
	t=–11.50	t=–3.69	t=–3.64	t=–4.00	t=–4.61	t=–1.75
	P<0.0001	P<0.01	P<0.01	P<0.001	P<0.001	P=0.10

The t statistic and two-tailed P-value for the partial regression slope are shown. Where P=0.034, it is noted whether the significant trend is an increase or decrease. That alpha level was chosen as a threshold for rejection of the null hypothesis to account for the increased Type I error rate from multiple tests on correlated data, as explained in the methods.

Table S2B. Changes in wing kinematics with increases in A_{horiz}, with the influence of V_{horiz} and A_{vert} held constant

	Cynopterus brachyotis (d.f.=17)	*Rousettus aegyptiacus* (d.f.=9)	*Pteropus pumilus* (d.f.=17)	*Eidolon helvum* (d.f.=17)	*Pteropus hypomelanus* (d.f.=17)	*Pteropus vampyrus* (d.f.=17)
Maximum wingspan (b_{max})	Increase				Increase	
	t=4.17	t=0.01	t=0.90	t=–1.12	t=3.19	t=–1.41
	P<0.001	P=0.99	P=0.38	P=0.28	P<0.01	P=0.18
Minimum Wingspan (b_{min})			Decrease			
	t=–0.89	t=–0.25	t=–3.29	t=–1.43	t=–1.59	t=0.13
	P=0.38	P=0.81	P<0.01	P=0.17	P=0.13	P=0.90
Wingbeat period (T)						
	t=–1.63	t=–1.18	t=–0.39	t=–0.56	t=–1.01	t=0.83
	P=0.12	P=0.27	P=0.70	P=0.58	P=0.33	P=0.42
Downstroke period (T_{down})						
	t=–0.81	t=–0.54	t=–1.67	t=–1.77	t=–1.82	t=0.61
	P=0.43	P=0.60	P=0.11	P=0.10	P=0.09	P=0.55
Downstroke Ratio (τ)						
	t=0.43	t=0.26	t=–2.04	t=–2.17	t=–2.27	t=0.14
	P=0.67	P=0.80	P=0.06	P=0.04	P=0.04	P=0.89
Wing stroke amplitude (ϕ)			Increase			
	t=1.49	t=–0.22	t=4.44	t=0.05	t=0.01	t=0.90
	P=0.16	P=0.83	P<0.001	P=0.96	P=1.00	P=0.38
Stroke plane angle (β)	Decrease	Decrease	Decrease	Decrease		
	t=–3.96	t=–3.85	t=–5.09	t=–3.06	t=–2.21	t=–1.43
	P<0.01	P<0.01	P<0.0001	P<0.01	P=0.04	P=0.18
Angle of attack (α)					Increase	
	t=–1.07	t=1.71	t=–1.78	t=–0.13	t=2.38	t=1.03
	P=0.30	P=0.12	P=0.09	P=0.90	P<0.034	P=0.32
α_1	Decrease		Decrease	Decrease		
	t=–4.10	t=–2.10	t=–5.02	t=–2.77	t=–0.26	t=–2.05
	P<0.001	P=0.07	P<0.001	P<0.034	P=0.80	P=0.06
α_2	Increase	Increase	Increase	Increase	Increase	Increase
	t=3.99	t=2.92	t=3.51	t=2.55	t=2.57	t=3.48
	P<0.001	P<0.034	P<0.01	P<0.034	P<0.034	P<0.01
Wing camber						
	t=0.85	t=–1.95	t=0.33	t=–0.56	t=1.62	t=0.75
	P=0.41	P=0.08	P=0.74	P=0.58	P=0.12	P=0.46
Strouhal number (St)	Increase		Increase	Increase		
	t=2.94	t=1.94	t=5.58	t=3.92	t=1.48	t=2.12
	P<0.01	P=0.08	P<0.0001	P<0.01	P=0.16	P=0.05
Lift coefficient (C_L)						Increase
	t=–1.18	t=–1.96	t=–1.78	t=0.05	t=0.46	t=2.57
	P=0.26	P=0.08	P=0.09	P=0.96	P=0.65	P<0.034

Table S2C. Changes in wing kinematics with Increases in A_{vert}, with the influence of V_{horiz} and A_{horiz} held constant

	Cynopterus brachyotis (d.f.=17)	*Rousettus aegyptiacus* (d.f.=9)	*Pteropus pumilus* (d.f.=17)	*Eidolon helvum* (d.f.=17)	*Pteropus hypomelanus* (d.f.=17)	*Pteropus vampyrus* (d.f.=17)
Maximum wingspan (b_{max})	Increase t=4.18 P<0.001	t=0.44 P=0.67	t=2.04 P=0.06	t=1.10 P=0.29	Increase t=3.20 P<0.01	t=–0.97 P=0.35
Minimum wingspan (b_{min})	t=0.31 P=0.76	t=0.76 P=0.47	t=–0.64 P=0.53	t=–1.17 P=0.26	t=0.09 P=0.93	t=0.14 P=0.89
Wingbeat period (T)	t=–2.19 P=0.04	Decrease t=–4.24 P<0.01	t=–0.26 P=0.80	t=–0.93 P=0.37	t=–1.30 P=0.21	t=0.29 P=0.77
Downstroke period (T_{down})	t=–1.26 P=0.23	t=–1.12 P=0.29	t=–0.31 P=0.76	t=–1.47 P=0.16	t=–0.44 P=0.66	t=0.68 P=0.51
Downstroke ratio (τ)	t=0.38 P=0.71	t=2.13 P=0.06	t=–0.09 P=0.93	t=–1.49 P=0.15	t=0.74 P=0.47	t=1.01 P=0.33
Wing stroke amplitude (ϕ)	t=–0.38 P=0.71	t=0.15 P=0.89	t=0.21 P=0.84	t=1.11 P=0.28	t=–1.86 P=0.08	t=0.34 P=0.74
Stroke plane angle (β)	t=–0.11 P=0.91	t=0.80 P=0.44	t=0.68 P=0.51	t=–1.76 P=0.10	t=0.91 P=0.37	t=–0.41 P=0.69
Angle of attack (α)	Increase t=2.55 P<0.034	t=2.12 P=0.06	t=0.63 P=0.54	t=–0.57 P=0.57	t=1.88 P=0.08	t=0.89 P=0.39
α_1	t=0.85 P=0.41	t=1.20 P=0.26	t=0.19 P=0.85	Decrease t=–2.73 P<0.034	t=1.03 P=0.32	t=–1.52 P=0.15
α_2	t=0.58 P=0.57	t=0.67 P=0.52	t=0.19 P=0.85	t=2.06 P=0.06	t=0.51 P=0.62	Increase t=2.72 P<0.034
Wing camber	t=2.18 P=0.04	t=1.31 P=0.22	t=1.35 P=0.19	t=2.15 P=0.05	Increase t=3.08 P<0.01	t=1.18 P=0.26
Strouhal number (St)	t=0.20 P=0.84	t=2.26 P=0.05	t=–0.57 P=0.58	Increase t=4.01 P<0.001	t=0.25 P=0.80	t=1.06 P=0.31
Lift coefficient (C_L)	Increase t=5.32 P<0.0001	Increase t=2.98 P<0.034	Increase t=5.24 P<0.0001	t=1.48 P=0.16	Increase t=5.97 P<0.0001	Increase t=3.77 P<0.01